Teknillinen korkeakoulu. Konetekniikan osasto. LVI-tekniikan laboratorio. A
Helsinki University of Technology. Department of Mechanical Engineering.
Laboratory of Heating, Ventilating and Air Conditioning. A
Espoo 2005

PERFORMANCE ANALYSIS OF HEAT TRANSFER PROCESSES FROM WET AND DRY SURFACES: COOLING TOWERS AND HEAT EXCHANGERS

REPORT A10

Ala Ali Hasan

Dissertation for the degree of Doctor of Science in Technology to be presented with due permission of the Department of Mechanical Engineering, Helsinki University of Technology for public examination and debate in Auditorium E at Helsinki University of Technology (Espoo, Finland) on the 6th of May, 2005, at 12 noon.

Helsinki University of Technology
Department of Mechanical Engineering
Laboratory of Heating, Ventilating and Air Conditioning

Distribution:

Helsinki University of Technology
HVAC-Library
P.O. Box 4100
FI-02015 TKK
Tel. +358 9 451 3601
Fax. +358 9 451 3611

Author's address:
Helsinki University of Technology
Laboratory of Heating, Ventilating and Air Conditioning
P.O. Box 4400
FI-02015 TKK
Tel. +358 9 451 3598
Fax. +358 9 451 3418
E-mail: ala.hasan@tkk.fi

Supervisor:
Professor Kai Sirén
Helsinki University of Technology

Reviewers:
Associate Professor David S-K Ting
University of Windsor, Canada
Department of Mechanical, Automotive and Materials Engineering

Dr. Pertti Heikkilä
Metso Paper Inc., Finland
Air Systems

Opponents:
Professor Mats Westermark
Royal Institute of Technology, Sweden
Department of Chemical Engineering and Technology

Dr. Pertti Heikkilä
Metso Paper Inc., Finland
Air Systems

ISBN 951-22-7634-8 (PDF)
ISBN 951-22-7633-X (printed)
ISSN 1238-8971

Otamedia Oy
2005

ABSTRACT

The objective of this work is to study the thermal and hydraulic performance of evaporatively cooled heat exchangers, including closed wet cooling towers, and dry tube heat exchangers with various geometries. Applications utilising such equipment exist in almost every thermal process. The investigation includes theoretical analysis, computational approaches, and experimental measurements.

In this work, a computational model is presented for the thermal performance of closed wet cooling towers intended for use in conjunction with chilled ceilings in cooling of buildings. A variable spray water temperature inside the tower is assumed. A prototype tower was subjected to experimental measurements to find its characteristics. Optimisation of the tower geometry and flow rates for specified design conditions is carried out in order to achieve a high value of the coefficient of performance (COP). Results from a global simulation program (including the tower model, a transient building model, a chilled ceiling model, system control etc.) show that closed wet cooling towers can be used with chilled ceilings to achieve acceptable indoor air temperatures in locations having suitable climatic conditions. This is supported by published results from a performance test of an office building using this method of cooling.

Simplification of the model is obtained by assuming a constant temperature for the spray water. The tower performance predicted by the simplified model and the computational model shows comparable results. The results of the simplified model are then incorporated with Computational Fluid Dynamics (CFD) to assess the temperature distribution inside the tower. It is shown that CFD can be implemented to study the effect of air distribution inside the tower on its performance.

The effect of introducing plate fins in evaporatively cooled plain circular tubes is experimentally studied. The measurement results show a 92% to 140% increase in the amount of heat transfer for the finned tubes. This is accompanied by an increase in the pressure drop, so that an indication of the combined thermal hydraulic performance is found to be close for the two geometries. However, it shows higher heat transfer rates per volume for the finned tubes. The performance of oval tubes in the evaporatively cooled heat exchanger is then experimentally investigated. The measurement results for the oval tubes show good heat and mass transfer characteristics; its average mass transfer Colburn factor is 89% of that for the circular tubes. Furthermore, it shows low friction factor for the air flow, which is 46% of that for the circular tubes. It is concluded that the tested oval tube is better than the circular tubes in combined thermal hydraulic performance.

The features of oval tubes appear clearer in a dry heat transfer process. Five shapes of dry oval tubes are experimentally investigated in a cross-flow of air. The measurement results for the oval tubes are compared with those for an equivalent circular tube. It is found that the Nusselt numbers Nu_D for the studied tubes are close for Reynolds numbers $Re_D < 4000$. While for higher Re_D, the Nu_D decreases with the increase of the

oval tube axis ratio. The drag measurements indicate lower drag coefficients $C_{d\ avg}$ for the oval tubes. It is revealed that the investigated oval tubes have favourable combined thermal-hydraulic performance, which is expressed in terms of (Nu_D /$C_{d\ avg}$). The ratio of (Nu_D /$C_{d\ avg}$) for the oval tubes to that for the circular tube is from 1.3 to 2.5.

PREFACE

"The highest reward for a person's toil is not what they get for it, but what they become by it"
John Ruskin, English poet (1819 - 1900)

This thesis is based on research work carried out at the Laboratory of Heating Ventilating and Air Conditioning, Helsinki University of Technology during the period 1998-2002. The work on the closed wet cooling tower relates to the ECOCOOL project (Ecological cooling for buildings by combining a closed wet cooling tower with chilled ceilings), which was partially funded by the Commission of the European Union (DGXII)- Joule IV programme. The work on dry oval tubes is part of the oval tube project, which was funded by the Finnish Technology Agency (TEKES) and the companies: Cetetherm Oy, Ekocoil Oy and Koja Oy. Additionally, I received grants from the L.V.Y Foundation and K. V. Lindholm Foundation. I would like to gratefully acknowledge all those parties for their funding.

I wish to express my deepest gratitude to my supervisor Professor Kai Sirén, who gave me the chance to come and work in the Laboratory and pursue my postgraduate study. I am grateful to him for all of his invaluable support during my work with him, and I would like also to thank him very much for his supervision and guidance through the work of this thesis.

I would like to sincerely thank the head of the HVAC Laboratory, Professor Olli Seppänen, for his support of my work and study in the Laboratory.

I would like to express my gratitude to pre-examiners Associate Professor David S-K Ting and Dr. Pertti Heikkilä for reviewing this thesis and for their valuable comments. I would also like to thank Professor Mats Westermark for acting as opponent during the discussion of this thesis.

I would like to thank the manager of the laboratory, Markku Sivukari, and the laboratory technician, Petteri Kivivuori, for their help in the experimental test facilities.

My thanks go to co-author Dr. Guohui Gan for his fruitful cooperation. Many thanks go to all of my colleagues in the HVAC Laboratory. Special thanks to Tapio Helenius for his support and guidance during my first days in Finland and to Mikko Suokas for his cooperation in the ECOCOOL project. Thanks to the staff of the Aerodynamics Laboratory who helped me in the turbulence intensity measurements. Additionally, my special thanks are to my colleagues Juha Jokisalo, Rauno Holopainen and Loay Saeed.

No words are able to express how grateful I am to my wife Khloud for all of her love and care and for her continuous encouragement, without which this work would not have been achievable. I would like also to mention my children, Mohammed, Hussain and Abdulla; with them this work was difficult to accomplish, but without them there would be no meaning in life.

I dedicate this work to the memory of my father, who would have been happy to see me on the stage with my thesis, and to my dear mother.

Finally, and before all, praise be to God, the most compassionate, the most merciful.

Ala

NOMENCLATURE

ABBREVIATIONS

COP	coefficient of performance
CWCT	closed wet cooling tower
ECHE	evaporatively cooled heat exchanger

SYMBOLS

A	area (m^2)
A_f	fin area (m^2)
A_i	inner area of a tube (m^2)
A_o	outer area of a tube (m^2)
c	outer major axis or chord (m)
C_d	drag coefficient, $C_d = F_d / (0.5 \rho V_T^2 A_F)$
C_H	specific heat capacity of moist air (J /(kg dry air K))
C_w	specific heat capacity of water (J kg^{-1} K^{-1})
d	tube inside diameter (m)
D	tube outside diameter (m)
Dif	diffusivity (m^2 s^{-1})
D_o	outside diameter for a circular tube, for an oval tube it is the outside diameter of a circular tube having equivalent perimeter, (m)
f	friction factor, $f = \Delta p / (0.5 \rho v_{max}^2)$
F_d	drag force (N)
G_a	air mass velocity (kg dry air s^{-1} m^{-2})
h_a	enthalpy of moist air (J /kg dry air)
h'_a	enthalpy of saturated air (J /kg dry air)
h_{fg}	latent heat of evaporation of water (J kg^{-1})
h'_i	enthalpy of saturated air at the interface temperature t_i (J /kg dry air)
h'_s	enthalpy of saturated air at the spray water temperature t_s (J /kg dry air)
H_a	humidity ratio of moist air (kg water/kg dry air)
H'_i	humidity ratio of saturated air at the interface temperature t_i (kg water/kg dry air)
H'_s	humidity ratio of saturated air at the spray water temperature t_s (kg water/kg dry air)
j_m	mass transfer Colburn factor, $j_m = K Sc^{2/3} / (\rho v_{max})$
k_a	thermal conductivity of air (W m^{-1} K^{-1})
k_w	thermal conductivity of tube wall (W m^{-1} K^{-1})
k_x	convective mass transfer coefficient (m s^{-1})
K	mass transfer coefficient (kg water s^{-1} m^{-2} (kg water/kg dry air) $^{-1}$)
L	tube length (m)
m_a	air mass flow rate (kg dry air /s)
m_c	cooling water mass flow rate (kg s^{-1})
m_h	hot water mass flow rate (kg s^{-1})
m_s	spray water mass flow rate (kg s^{-1})
Nu	Nusselt number, $Nu = \alpha_a D / k_a$
Nu_D	mean Nusselt number for a tube, $Nu_D = \alpha_a D_o / k_a$

q_a	rate of heat transfer for air (W)
q_c	rate of heat transfer for cooling water (W)
q_f	rate of heat transfer from a fin (W)
q_h	rate of heat transfer for hot water (W)
q_s	rate of heat transfer for spray water (W)
R	nominal axis ratio for an oval tube
Re	Reynolds number, Re = $v\ D\ \rho\ /\ \mu$
Re_c	Reynolds number, $Re_c = V_T\ c\ \rho\ /\ \mu$
Re_D	Reynolds number, $Re_D = V_f\ D_o\ \rho\ /\ \mu$
Sc	Schmidt number, Sc = $\mu\ /\ (\rho\ Dif)$
Sh	Sherwood number, Sh = $k_x\ D\ /\ Dif$
t_a	air temperature (°C)
t_c	cooling water temperature (°C)
t_h	hot water temperature (°C)
t_i	air-spray water interface temperature (°C)
t_s	spray water temperature (°C)
Tu	turbulence intensity
U_o	overall heat transfer coefficient (W m^{-2} K^{-1})
v_{max}	velocity of air at minimum flow section (m s^{-1})
V_f	free stream velocity of air (m s^{-1})
V_T	upstream velocity of air to test section (m s^{-1})
y	outer minor axis of an oval tube (m)
α_a	air side convective heat transfer coefficient (W m^{-2} K^{-1})
α_c	convective heat transfer coefficient between cooling water and tube wall (W m^{-2} K^{-1})
α_h	convective heat transfer coefficient between hot water and tube wall (W m^{-2} K^{-1})
α_i	convective heat transfer coefficient for the airside of the interface (W m^{-2} K^{-1})
α_s	convective heat transfer coefficient between spray water and tube wall (W m^{-2} K^{-1})
μ	dynamic viscosity (kg s^{-1} m^{-1})
ρ	density (kg m^{-3})

Subscripts

a	air
c	cooling water
h	hot water
lm	log-mean-difference
s	spray water
1	inlet to tower
2	outlet of tower

Superscript

´	saturated condition

TABLE OF CONTENTS

LIST OF PUBLICATIONS

I Hasan A, Sirén K (2002). Theoretical and computational analysis of closed wet cooling towers and its applications in cooling of buildings, *Energy and Buildings* **34** (5): 477–486.

II Hasan A, Gan G (2002). Simplification of analytical models and incorporation with CFD for the performance prediction of closed wet cooling towers, *International Journal of Energy Research* **26** (13): 1161–1174.

III Hasan A, Sirén K (2003). Performance investigation of plain and finned tube evaporatively cooled heat exchangers, *Applied Thermal Engineering* **23** (3): 325–340.

IV Hasan A, Sirén K (2004). Performance investigation of plain circular and oval tube evaporatively cooled heat exchangers, *Applied Thermal Engineering* **24** (5-6): 777–790.

V Hasan A (2004). Thermal-hydraulic performance of oval tubes in a cross-flow of air, accepted for publication in *Heat and Mass Transfer*.

The disputant is the principal author of the five publications. In Publication II, the author carried out the work of simplifying the analytical models and comparing the results of the prototype tower with those from the computational model. The co-author, Dr. Guohui Gan, carried out the CFD simulations. The analysis of the results and the conclusions were worked out together. The TRNSYS simulation in Publication I was carried out by Mikko Suokas as part of the Laboratory contribution within the ECOCOOL project.

1 INTRODUCTION

Evaporatively cooled heat exchangers (ECHEs) have many applications in the fields of air-conditioning, refrigeration and power plants. They can achieve higher heat transfer rates than dry heat exchangers. Heat transfer takes place from a hot fluid flowing inside the tubes of the heat exchanger to air through a water film which is formed by spraying water onto the heat exchanger surface. Closed wet cooling towers (CWCTs), evaporative fluid coolers and evaporative condensers are examples of this application. Evaporative fluid coolers usually operate at higher temperature levels than closed wet cooling towers (CWCTs); however the thermal analysis is similar. Evaporative condensers work at a constant condensing temperature. In cases in which the load is relatively low, dry operation of an evaporatively cooled heat exchanger could be sufficient to achieve the thermal duty. Additionally, cross-flow dry-surface heat exchangers are widely used in numerous applications.

The rate of heat transfer could be increased from dry and wet surface heat exchangers by improving the geometry of the surfaces. An example is the use of fins or noncircular tubes, which increases the compactance of the exchanger. With higher contact surfaces, the accompanied energy required to move air across the surfaces will typically increase. Thus, the energy efficiency of the heat transfer process is an important parameter that has to be studied too.

1.1 Background

Evaporatively cooled heat exchangers

Due to their large surface area, chilled ceilings can work with a low temperature difference between room air and the surface of the cooling panel. This results in lower air velocities in the room, so a high level of indoor air comfort can be provided for the occupants. When compared to conventional systems, chilled ceilings require a smaller volume for the distribution system; besides this, the ventilation rate can be reduced to lower levels. The use of water as the thermal carrier medium instead of air results in a reduction in the energy demanded for the fluid pumping. For this reason, energy required to pump water in a water-based cooling system is lower than that required to blow air in an air-based system. With chilled ceilings, the cooling effect could be achieved by a relatively high cooling water temperature. A cooling water supply temperature of 18°C (Sprecher et al., 2000) or about 18 - 20°C (Koschenz, 1995; Facão and Oliveira, 2000) could be used; this could be supplied from a CWCT.

Three fluids flow inside a CWCT: cooling water, spray water, and air. The cooling water comes from the chilled ceiling and flows inside tubes arranged in rows inside the tower. Spray water is injected onto the tube surfaces and is recirculated in a closed circuit. It is an intermediate fluid in the heat transfer process. Heat carried away from the building by the cooling water transfers to the spray water through the tube walls.

From the spray water, it transfers to air by both sensible heat and latent heat. The latter makes the major contribution and is caused by the evaporation of a small amount of the spray water into the air stream. The use of the closed type of cooling towers, which is indirect contact equipment, permits a high level of cleanliness in the piping, resulting in effective internal heat transfer surfaces, reduced maintenance costs, and longer operational life.

A system consisting of a closed wet cooling tower and chilled ceilings when used for the cooling of buildings will result in a Chlorofluorocarbon (CFC) free and environmentally clean system. The initial and running costs of the system are low when compared to traditional vapour-compression cooling systems. Figure 1.1 shows the basic components of the cooling system, while Figure 1.2 shows the CWCT schematic. Making use of the natural cooling effect, the CWCT brings down the cooling water temperature to lower levels, which depend on the outdoor air conditions and the effectiveness of the heat transfer process. The wet bulb temperature is, theoretically, the lowest temperature for any air-water contact operation, which could be reached only under the adiabatic condition "adiabatic saturation". The wet bulb temperature for many locations in Europe may permit use of the proposed cooling system. An example is given in Fig. 1.3 by showing the percentage occurrence of wet bulb temperature in Zurich (CH), which is based on hourly test-reference-year data. The percentage occurrence is defined as the percentage of the total annual hours (8760 h) during which a temperature at or below a particular temperature occurs.

CWCTs are conventionally used for industrial applications in a temperature range of 32-46 °C. Towers sized for industrial applications will cause overpowering in air and spray water flow when used with chilled ceilings in cooling of buildings (Sprecher et al., 1996). This implies that a CWCT intended for such an application should be designed according to empirical data obtained in the range of the operating temperatures.

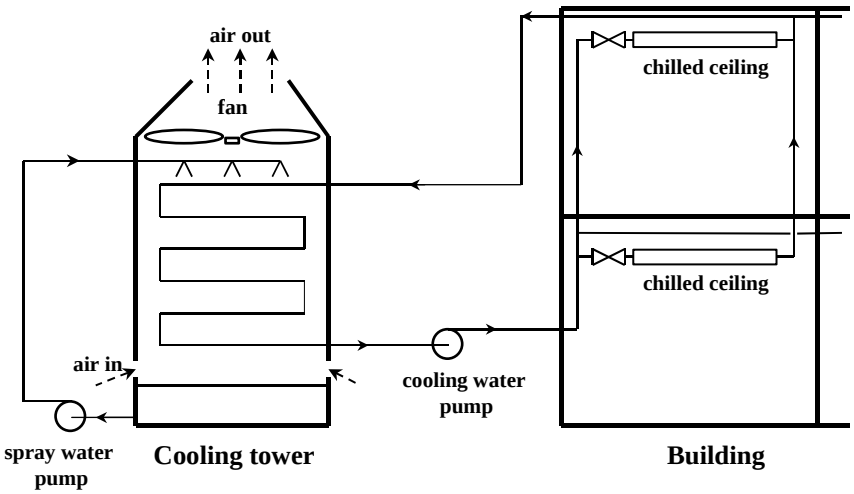

Fig. 1.1. The components of the cooling system.

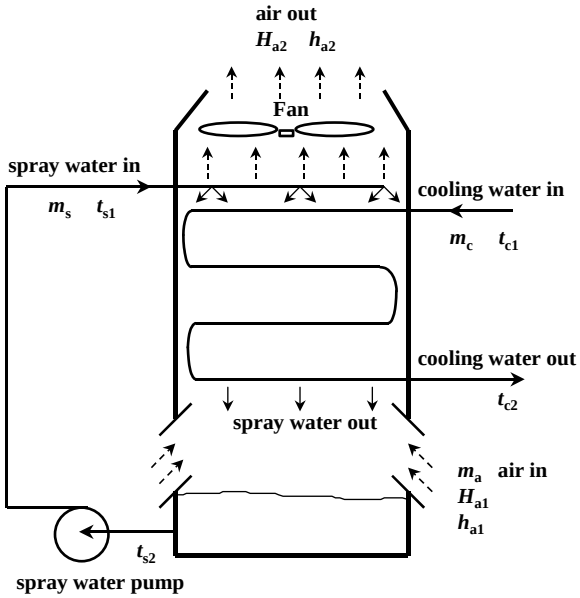

Fig. 1.2. A closed wet cooling tower (CWCT).

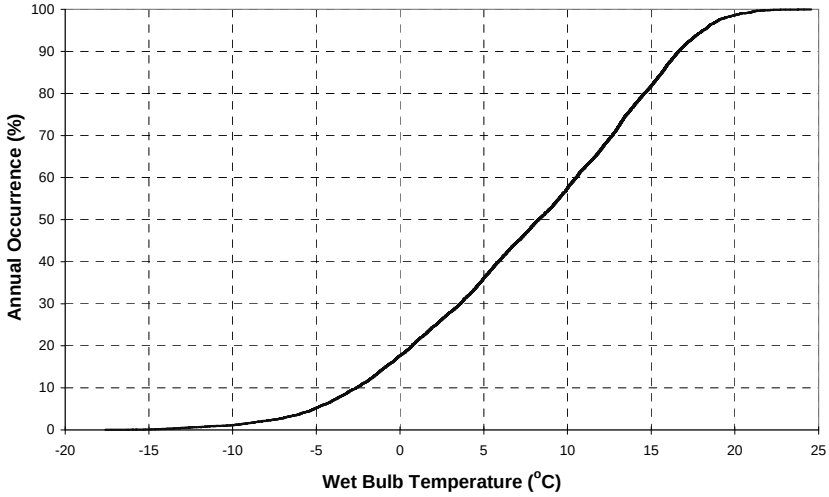

Fig. 1.3. Percentage annual occurrence of wet bulb temperature in Zurich (CH).

Fluid flow in an ECHE involves simultaneous heat and mass transfer that is regulated by the relevant heat and mass balance equations. Parker and Treybal (1962) presented an analytical method for evaporative liquid coolers. The spray water temperature variation along the heat exchanger was considered. The solution of the governing differential equations was achieved by assuming a linear relation between the spray water temperature and enthalpy of the saturated air-water mixture. The heat and mass transfer coefficients were needed for the solution of the temperature and humidity distribution. The transfer coefficients were found from experimental measurements.

Mizushina et al. (1967) conducted tests on the cores of an evaporative cooler with three different tube diameters. An assumption of constant spray water temperature inside the tower was applied to evaluate the empirical heat and mass transfer correlations. The results of the mass transfer coefficient were presented in terms of the air and spray water Reynolds numbers. In another paper, Mizushina et al. (1968) set the design limitations for evaporative liquid coolers where the general case of variable spray water temperature inside the tower was considered. The saturation enthalpy of air was assumed as a linear relation with the spray water temperature, while the evaporation of spray water was ignored.

Niitsu et al. (1969) tested banks of plain and finned tubes. The tubes were in a staggered arrangement. Correlations of the plain tubes and the finned tubes were presented.

Peterson et al. (1988) applied transfer coefficients estimated according to the Parker and Treybal's correlation (1962) to determine the performance of plain tubes. Field tests on an evaporative condenser were performed, and the predicted and measured results were compared, showing a 30% underprediction in the heat load which was attributed to low estimated values of the overall heat transfer coefficient.

Dreyer and Erens (1990) carried out experimental work on plain tubes in a cross-flow arrangement and compared the heat and mass transfer coefficients with a counter-flow arrangement. For CWCTs, counter-flow arrangement refers to multiple passes of the same tube across the heat exchanger where air flows across the tubes, which is not a purely counter flow.

Koschenz (1995) presented a model for CWCTs to be used with chilled ceilings. Two assumptions were implemented: first, a constant spray water temperature along the tower; second, the spray water temperature was equal to the outlet cooling water temperature. He calculated the outlet cooling water temperature according to his model and compared it with data from a manufacturer's catalogue. He indicated that the agreement between the results was fully satisfactory for practical applications.

Zalewski and Gryglaszewski (1997) presented a mathematical analytical model for the heat and mass transfer equations for evaporative fluid coolers. The analogy between heat and mass transfer was applied to find the mass transfer coefficient from heat transfer correlations of fluid flow across tube bundles. A correction for the mass transfer coefficient was suggested as a function of inlet air wet bulb temperature to improve agreement between calculated data and experimental results for an evaporative cooler.

Jang and Wang (2001) presented a numerical model for closed-type cooling towers with bare tube banks. The heat and mass transfer coefficients were calculated according to correlations from other works. Experimental work with 60°C inlet water temperature was carried out. The results show that a counter flow of air and spray water has a 10% higher overall heat transfer coefficient than that of a parallel flow. The disagreement between the numerical predictions and experimental data was 20-25%.

Computational fluid dynamics (CFD) has been implemented in the analysis of the operation of cooling towers. Milosavljevic and Heikkilä (2001) implemented CFD to predict the air flow pattern inside a counter flow open type cooling tower sized for industrial applications. The differences in air velocity upstream of the tower's filling material were found to be < 5%. Furthermore, CFD was implemented to assess the effect of external air flow around the tower and the backflow in different weather conditions.

CFD has also been implemented to study the temperature and air flow fields in CWCTs. Boundary conditions, such as heat flux distribution along the cooling tower, have a significant influence on the prediction of the thermal performance. Gan and Riffat (1999) applied CFD to predict the performance of a CWCT assuming a uniform volumetric heat flux in the tube coils. The results showed an increase of the cooling water temperature for the lower tube rows, which was attributed to the assumption of uniform heat flux generation. In reality, the heat flux is higher for the upper rows because of the higher inlet cooling water temperature. In another paper, Gan et al. (2001) assumed a linear heat flux distribution along the tower, which was twice as high for the upper rows as for the bottom rows. In a conclusion of the analysis for the pressure field, the predicted pressure losses for a single-phase flow of air over the tubes were in good agreement with estimated values from empirical equations. For the thermal performance of the tower, it was concluded that any assumed heat flux distribution would yield inaccurate results. Therefore, CFD needs to be incorporated with thermal models describing the heat flux distribution inside the tower.

Finned tube evaporatively cooled heat exchangers

Niitsu et al. (1969) tested banks of finned tubes in evaporative liquid coolers. The tubes were 16 mm o. d. in a staggered arrangement with a transversal tube spacing of 37.5 mm and longitudinal tube spacing of 38.1 mm. The fins were circular, 42.6 mm diameter. Two fin spacings were tested (6.1 mm and 11 mm). They concluded that the finned bank had much lower heat and mass transfer coefficients for the spray water side compared to the plain bank. This was attributed to possible water hold up between the fins and low fin efficiency for the wet fins (Finlay and Harris, 1984).

Kried et al. (1978) proposed a theoretical model for deluged (flooded) finned heat exchangers. By introducing appropriate parameters, they transformed wet-surface heat transfer equations to approximated equations that were in analogy to dry heat transfer equations.

Leidenfrost and Korenic (1986) presented a mathematical model for finned tube evaporative condensers based on a graphical procedure, which was executed by a computer program in a stepwise integration. Mass transfer coefficients were estimated from dry heat transfer coefficients.

Erens (1988) numerically compared three different designs for an evaporative liquid cooler. The first design with plain tubes, the second with the tubes placed integrally in a plastic fill, and the third with the plastic fill placed below the tube bank. The calculation results indicated that the performance of the plain tube cooler could be considerably enhanced by the utilisation of the fill material.

To the disputant's knowledge, only Niitsu et al. (1969) has presented a comparison of the performance of plain circular tubes and these tubes after being finned. The literature lacks more data for such comparisons.

Oval tube heat exchangers

If a heat exchanger is constructed from oval tubes (where the major axis is parallel to air flow), the expected pressure drop of air will be low. This is due to the slender shape of an oval tube. The lower pressure drop will result in a decrease in the pumping power required to move air across the tubes.

The disputant couldn't find any publication in the open literature about the utilisation of oval tubes in evaporatively cooled heat exchangers. However, a catalogue of Evapco Inc. (www.evapco.com), manufacturer of cooling towers, evaporative liquid coolers and evaporative condensers shows that some of the company's products are manufactured according to a patented Thermal-Pak® coil design in which elliptical tubes are utilised. Enough information is not available about this design.

Dry operation of an ECHE could bring the temperature of the process fluid to the required level when the thermal load is relatively low. In addition, dry heat exchangers have plenty of applications in various fields.

Dry oval tubes have been subjected to experiments for a long time. Maybe the oldest work on a single elliptical cylinder mentioned in the literature is that by Reiher (1925), as quoted by Ota et al. (1983), who reported the mean heat transfer coefficient for an elliptical cylinder whose configuration was obscure.

Ota et al. (1983) investigated experimentally the thermal performance of a single elliptical cylinder with an axis ratio (major axis to minor axis) of 2. The Reynolds number (Re_c) was 5000 to 90000 (where Re_c is the air Reynolds number based on the major axis c) and the angle of attack was 0 to 90˚. For air flow parallel to the major axis, they indicated that the Nusselt number for the elliptical cylinder was higher than that obtained for a circular cylinder from an empirical correlation by Hilpert (1933).

Ota et al. (1984) tested an elliptical cylinder with an axis ratio of 3, with Re_c from 8000 to 79000. They indicated that the measurements for the Nusselt number were higher than those for a circular cylinder from Hilpert's correlation. Their comparison of the results with those from the previous work on the elliptical cylinder with axis ratio 2 (Ota et al., 1983) showed a small increase in heat transfer.

Kondjoyan and Daudin (1995) studied experimentally the effect of variation in the free stream turbulence intensity Tu from 1.5% to 40% on the heat transfer from a circular cylinder and an elliptical cylinder (axis ratio 4). The air Reynolds number Re_D was between 3000 and 40000, where Re_D is based on the diameter of an equivalent circular cylinder. Their conclusion was that turbulence intensity effect is as important as the air velocity effect. However, they indicated that the Nusselt number for the elliptical cylinder was about 14% lower than that for the equivalent circular cylinder.

For the flow around an elliptical cylinder, Schubauer (1936) made measurements of the velocity distribution inside the laminar boundary layer. Hoerner (1965) showed the drag coefficient as a function of the axis ratio.

For more than one tube or for a bank of tubes, Merker and Hanke (1986) carried out experimental work for the heat transfer and pressure drop of staggered oval tube banks with different transversal and longitudinal spacings. The axis ratio of the oval tube was 3.97. They indicated that oval tubes in a heat exchanger will have a smaller frontal area on the shell-side compared to circular tubes.

Ota and Nishiyama (1986) experimentally studied the flow around two elliptical cylinders (axis ratio 3) which were in a tandem arrangement. The static pressure distribution on the surface was measured and the drag, lift, and moment coefficients were evaluated for a range of angles of attack and cylinder spacings. They concluded that the flow characteristics vary drastically with the angle of attack and cylinder spacing.

Nishiyama et al. (1987) investigated the heat transfer around four elliptical cylinders (axis ratio 2) that were placed in a tandem arrangement with air Reynolds number Re_c from 15000 to 70000. They showed that the thermal performance of the elliptical cylinders was comparable to that of in-line circular cylinders at narrower cylinder spacings and at smaller angles of attack.

Salazar et al. (1997) measured the heat transfer from a bank of elliptical tubes in a cross flow. The axis ratio of the elliptical tube was 1.054, 1.26, and 1.44. The results were presented in terms of Reynolds number and Nusselt number where the elliptical tube minor axis was considered as the characteristic length. The results indicated that correlations of circular tubes were slightly higher than their measurements for the elliptical tubes.

It could be noted that the characteristic length in the non-dimensional parameters (e.g. Re and Nu) has been selected in different ways by the researchers worked on oval tubes, as it was taken as the major axis c, the minor axis y or the diameter of the equivalent circular cylinder D_o.

For colder elliptical tubes that cool warmer air flowing normal to the tubes, Liu et al. (2003) and Khan et al. (2004) examined experimentally the performance of an array of 18 elliptical tubes, where the tube axis ratio was 3.33. Correlations for the Nusselt

number on the water side and air side were presented in terms of the relevant Reynolds numbers and the dimensionless pressure drop factor on the air side was evaluated.

For finned elliptical tubes there are several experimental works: Brauer (1964) and Schulenberg (1966) showed better heat transfer for finned elliptical tubes than for finned circular tubes, and Saboya and Saboya (2001) indicated no major differences, while Jang and Yang (1998) indicated lower heat transfer performance for finned elliptical tubes.

As became apparent, the available literature seemed to be inconclusive concerning the expected thermal performance of oval tubes relative to circular tubes. While some works refer to better performance, others indicate the reverse. This has also been concluded by Castiglia et al. (2001). However, their experimental and numerical study for a widely spaced array of elliptic cylinders (axis ratio 2) covered only the flow field. Their results show that the flow was characterized by low turbulence levels and poor lateral mixing. From the flow field conclusion, they expect that the studied elliptic cylinders would not increase the rate of heat transfer when compared to circular cylinders.

Oval tubes in a cross-flow of air would exhibit lower air pressure drop than circular tubes. The operating costs in cross-flow heat exchangers are mainly due to the energy required to move air across the tubes. While the advantage gained from their hydraulic performance is clear, no special conclusions could be drawn from the available literature concerning the expected thermal performance of oval tubes relative to circular tubes.

1.2 Objectives

The general objective of this work is to study the heat transfer process from dry and wet surfaces for applications of evaporatively cooled heat exchangers, including closed wet cooling towers, and dry heat exchangers. The study shows the effect of improving the surface geometry on the heat transfer and investigates the feasibility of such processes in terms of energy efficiency.

Specific objectives of this study are:

- To present a general model for the thermal performance of CWCTs that takes into consideration the variation of the spray water temperature along the tower
- To develop a procedure for the optimisation of the CWCT dimensions and flow rates to achieve a specified thermal duty with high COP value
- To simulate building performance by a global building program that includes the CWCT's model
- To implement simplifications to the CWCT analytical model and compare the results with those obtained from the general model and experimental data

- To investigate CFD simulation of the tower's performance by incorporating the simple tower model and to study the effect of air flow distribution inside the tower on the performance
- To experimentally investigate the performance of plain tubes and finned circular tubes in evaporatively cooled heat exchangers and compare their thermal and hydraulic performance
- To experimentally study the thermal and hydraulic performance of plain oval tubes in evaporatively cooled heat exchangers and compare the performance with that of the plain circular tubes
- To test several shapes of oval tubes and a circular tube for dry heat transfer in a cross-flow of air, and compare their thermal and hydraulic characteristics

1.3 Contents

This thesis comprises five papers published in international scientific journals. Papers I to IV deal with heat and mass transfer in ECHEs, including CWCTs, while paper V covers an investigation into dry heat transfer from several shapes of oval tubes.

Paper I covers a theoretical and computational study on CWCTs, and investigates its applications in cooling of office buildings in combination with chilled ceilings. This is done by developing a general model for the thermal performance of CWCTs with a variable spray water temperature along the tower. Based on this, a computational model is developed. Experimental measurements for the operation of a prototype tower are considered to optimise the tower dimensions and flow rates for a required cooling load and to achieve high COP values. The tower model is integrated into a global system simulation program which includes the transient building performance program and models for other components of the cooling system. The global model simulates the system performance for different locations with different operating conditions and studies its energy performance and indoor air temperatures.

Paper II studies the effects of simplifications of the general model by considering a constant spray water temperature. The results are compared to those from the computational model and from experimental data. The simplified model is incorporated with CFD to assess the effects of air flow distribution inside the tower on the thermal performance of the tower.

Paper III investigates, experimentally, the performance of plain and finned circular tubes in an evaporatively cooled heat exchanger. The work is extended in Paper IV to cover the performance of plain oval tubes. The thermal and hydraulic performance is studied, which refers to the amount of heat transfer from the tubes and the accompanied pressure drop in the air flow across the tubes.

Paper V includes an experimental investigation of dry heat transfer in a cross-flow of air. Five oval tube shapes are studied and the thermal and hydraulic characteristics are compared with that for a circular tube having an equivalent surface area. The

investigation covers three plain oval tubes and two oval tubes with special configurations: a tube with two soldered wires, and a cut-oval tube.

The energy efficiency for each heat transfer process has been expressed in terms of appropriate physical parameters which refer to the accomplished thermal duty and the related energy demand.

New acquired knowledge from this thesis is about:

- Application of CWCTs, in combination with chilled ceilings, in cooling of office buildings: Such an application has not been investigated before
- Simplifications of CWCT models and their incorporation with CFD to study the effects on the thermal performance: Published literature for the implementation of CFD in the thermal and hydraulic design of CWCTs does not include incorporation of simple analytical models
- Effects of introducing plate fins in evaporatively cooled plain circular tubes on its thermal-hydraulic performance: There is only one comparable work (Niitsu et al., 1969) which indicates much lower heat and mass transfer coefficients for the spray water side and was attributed to possible water hold up between the fins
- Thermal-hydraulic performance of oval tubes in an evaporatively cooled heat exchanger: A similar work has not been found in the open literature
- Comparative thermal-hydraulic characteristics of five oval tubes and one circular tube in a cross-flow of air for dry heat transfer applications: Literature are inconclusive concerning the thermal performance of oval tubes in relation to circular tubes

2 THEORETICAL AND COMPUTATIONAL ANALYSIS OF CLOSED WET COOLING TOWERS AND ITS APPLICATIONS IN COOLING OF BUILDINGS

CWCTs could be used to provide cooling water to chilled ceilings in the cooling of buildings. The cooling water temperature achieved by the CWCT will depend on the temperature approach to the prevailing wet bulb temperature in the location. A cooling tower making use of the free cooling effect would show values of the coefficient of performance (COP) higher than that for a vapour compression machine. The objectives of paper I are to develop a general model for the thermal performance of CWCTs and to investigate the application of CWCTS with chilled ceilings in cooling of office buildings. The model could be used for the optimisation of the tower geometry and flow rates and for higher COP values. The model could be part of a cooling system simulation program which could include a transient building model.

2.1 Theoretical Background

As shown in Fig. 2.1a, three fluids flow inside a CWCT (cooling water, spray water, and air). The cooling water, coming from chilled ceilings, carries the heat from the building. The heat transfers from the cooling water to the spray water, from which it transfers to air. Taking an element of a tube, which has a length of dL and a surface area of dA, Fig. 2.1b shows the flow direction for the three streams inside the element. A one-dimensional steady-state analysis is assumed.

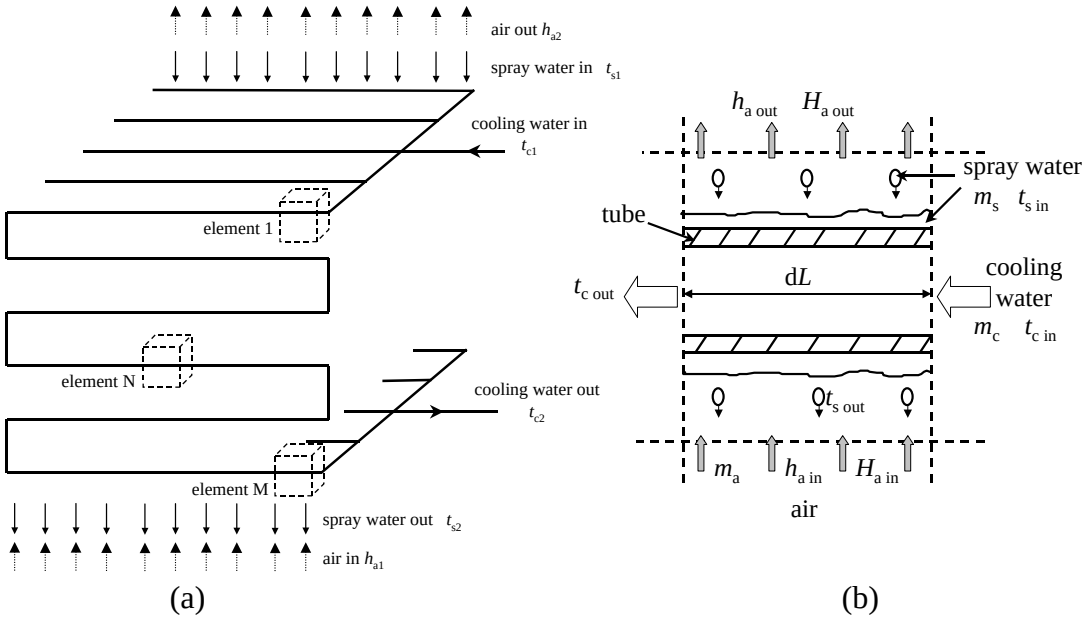

Fig. 2.1. Flow streams inside the tower

2.1.1 Energy balance

Heat transfer takes place from the cooling water through the tube wall to the spray water as a result of the temperature gradient. The rate of heat transfer from the cooling water $\mathrm{d}q_\mathrm{c}$ is

$$\mathrm{d}q_\mathrm{c} = m_\mathrm{c} C_\mathrm{w}\, \mathrm{d}t_\mathrm{c} = -U_\mathrm{o}(t_\mathrm{c} - t_\mathrm{s})\,\mathrm{d}A \tag{2.1}$$

U_o is the overall heat transfer coefficient based on the outer area of the tube. It accounts for the heat transfer coefficient between the cooling water and the internal surface of the tube α_c, the tube wall thermal conductivity k_w, and the heat transfer coefficient between the external surface of the tube and the spray water bulk α_s

$$\frac{1}{U_\mathrm{o}} = \frac{1}{\alpha_\mathrm{c}}\left(\frac{D}{d}\right) + \frac{D}{2k_\mathrm{w}}\ln\left(\frac{D}{d}\right) + \frac{1}{\alpha_\mathrm{s}} \tag{2.2}$$

α_c is taken from empirical correlation in literature. When α_s is considered as an input, it could be estimated from literature. Heat gained by the air stream $\mathrm{d}q_\mathrm{a}$ is due to heat transferred from the air-water interface, which results in an enthalpy rise of $\mathrm{d}h_\mathrm{a}$. $\mathrm{d}q_\mathrm{a}$ consists of sensible heat $\mathrm{d}q_\mathrm{sn}$ and latent heat $\mathrm{d}q_\mathrm{L}$.

$$\mathrm{d}q_\mathrm{a} = m_\mathrm{a}\mathrm{d}h_\mathrm{a} = \mathrm{d}q_\mathrm{sn} + \mathrm{d}q_\mathrm{L} \tag{2.3}$$

Substituting for the sensible and latent heats

$$\mathrm{d}q_\mathrm{a} = m_\mathrm{a}\mathrm{d}h_\mathrm{a} = \alpha_\mathrm{i}(t_\mathrm{i} - t_\mathrm{a})\mathrm{d}A + K(H'_\mathrm{i} - H_\mathrm{a})\,h_\mathrm{fg}\mathrm{d}A \tag{2.4}$$

where α_i is the heat transfer coefficient for the airside of the interface, K is the mass transfer coefficient, h_fg is the latent heat of evaporation of water, and H'_i is the humidity ratio of saturated moist air at the interface temperature t_i.

The enthalpy of moist air is h_a

$$h_\mathrm{a} = C_\mathrm{H}\, t_\mathrm{a} + h_\mathrm{fg} H_\mathrm{a} \tag{2.5}$$

where C_H is the specific heat capacity of humid air. $C_\mathrm{H} = C_\mathrm{a} + H_\mathrm{a}\, C_\mathrm{wv}$, where C_a and C_wv are the specific heat capacity of air and water vapour, respectively (ASHRAE, 1997). Substituting for t_a and t_i from Eq. (2.5) in Eq. (2.4) and rearranging the terms yields

$$m_a \mathrm{d}h_a = \left[\frac{\alpha_i}{C_H}(h_i' - h_a) + h_{fg} K (1 - \frac{\alpha_i}{K C_H})(H_i' - H_a) \right] \mathrm{d}A \tag{2.6}$$

where h_i' is the enthalpy of saturated air at the interface temperature t_i. Noting that the Lewis relation ($\alpha_i / K C_H$) appears on the right hand side of Eq. (2.6). The Lewis relation can be obtained from the Reynolds analogy, which gives ($\alpha_i / K C_H$) = $(\mathrm{Sc/Pr})^{2/3}$, where (Sc/Pr) is the Lewis number. For air-water vapour mixtures, $(\mathrm{Sc/Pr})^{2/3} \approx 1$. However, the approximation to unity involves only a small error (ASHRAE, 1997).

Hence, Eq. (2.6) can be reduced to

$$m_a \mathrm{d}h_a = K(h_i' - h_a)\,\mathrm{d}A \tag{2.7}$$

The thermal resistance of the liquid side of the interface could be considered negligible (ASHRAE, 1992), so that $t_i = t_s$. Therefore, the interface enthalpy h_i' in Eq. (2.7) equals h_s', the saturated air enthalpy at the spray water temperature t_s. Thus

$$\mathrm{d}q_a = m_a \mathrm{d}h_a = K(h_s' - h_a)\,\mathrm{d}A \tag{2.8}$$

Equation (2.8) is the Merkel equation (Merkel, 1925). It shows that the energy transfer could be represented by an overall process based on the enthalpy potential difference, between the air-water interface and bulk air, as the driving force.

The energy balance for the three streams flowing inside the element shown by Fig. 2.1b gives

$$\mathrm{d}q_c + \mathrm{d}q_a + \mathrm{d}q_s = 0 \tag{2.9}$$

The amount of variation in the spray water flow rate m_s, due to evaporation, is so small that m_s could be considered constant (ASHRAE, 1992). Hence, Eq. (2.9) becomes

$$m_c C_w \mathrm{d}t_c + m_a \mathrm{d}h_a + m_s C_w \mathrm{d}t_s = 0 \tag{2.10}$$

Spray water temperature varies inside the tower according to the height of the element. If the heat loss from the spray water piping outside the tower is considered negligible, the inlet spray water temperature t_{s1} will equal the outlet spray water temperature t_{s2}.

$$t_{s1} = t_{s2} \tag{2.11}$$

When applied to the whole tower, the term refering to dq_s will disappear from Eqs. (2.9 and 2.10).

2.1.2 Mass balance

The mass balance for the element gives the rate of spray water evaporation m_e (kg s^{-1})

$$m_e = m_a dH_a = K(H'_s - H_a)\,dA \tag{2.12}$$

Equations (2.1, 2.8, 2.10, 2.11, and 2.12) govern the heat and mass transfer process in the tower.

The Merkel equation (Eq. 2.8) is a result of the assumption of Lewis number = 1. Another general approach by Poppe (1973) takes the Lewis number in Eq. (2.6) without such an approximation. Erens and Dreyer (1988) implemented the two methods on a cross-flow wet liquid cooler. Their calculations for a 640 kW liquid cooler showed insignificant differences between the results obtained by these two methods. This was confirmed by them later (Dreyer and Erens, 1990) according to measurement results from an evaporative liquid cooler.

2.2 Computational model solution

The solution involves dividing the tower into elementary volumes where the properties of cooling water, spray water, and air are defined on the surface boundaries of the elements, as shown in Fig. 2.1b. The exchanged data between the adjacent elements depend on the direction of the flow: horizontally for the cooling water, and vertically for the spray water (downward) and the air (upward).

The solution starts by taking the first element uptower, surrounding the tube at the cooling water inlet, and proceeds in the direction of the cooling water flow. Iterative methods should be implemented because of the scatter of the tower's inlet parameters uptower and downtower. Figure 2.2 shows the flowchart diagram for the temperature field solution. Finite difference representation of Eqs. (2.1, 2.8, and 2.10), together with Eq. (2.11), is implemented. Successive iterations are needed for the values of the outlet air enthalpy h_{a2} and the inlet spray water temperature t_{s1} to find the temperature for all the elements. Subsequently, the solution for the humidity distribution can be found from Eq. (2.12) starting from the last downtower element upwards.

2.3 Results and discussion

A prototype tower with a design cooling power of 10 kW was manufactured by Sulzer-Escher Wyss GmbH Lindau (DE) to operate with chilled ceilings for the purpose of

cooling of buildings as part of the activities of the ECOCOOL project (http://paginas.fe.up.pt/~jfacao/ecocool/). Dimensions of the prototype tower are shown in Fig. 2.3.

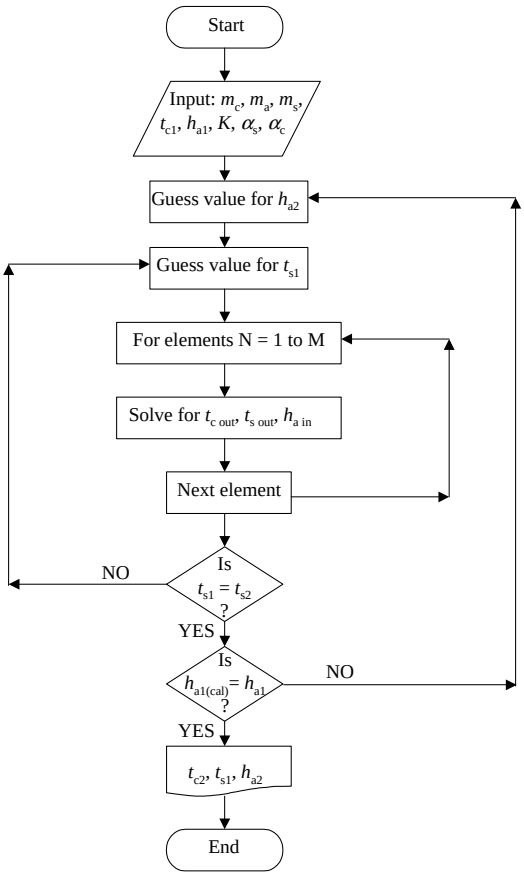

Fig. 2.2. Flow chart diagram for the temperature distribution calculation.

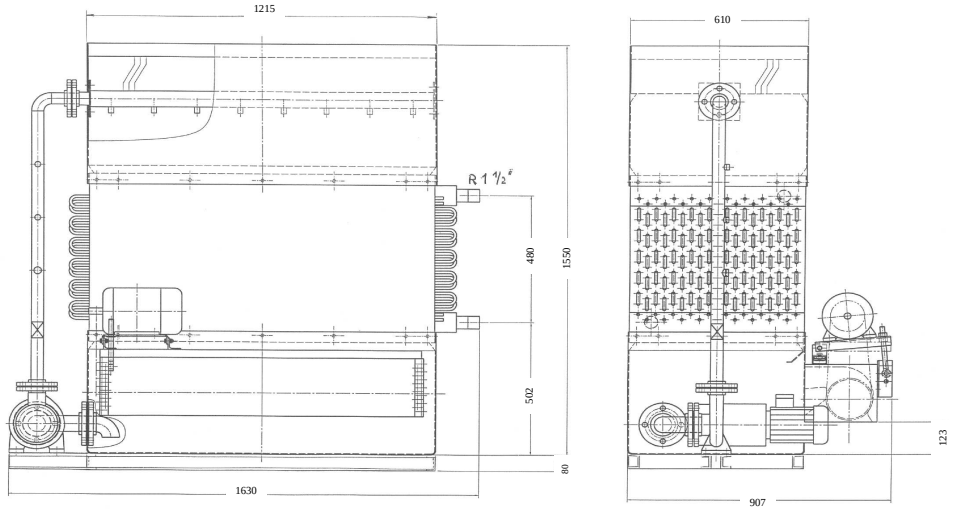

Fig. 2.3. The prototype tower dimensions (in mm).

The tower consists of 19 tubes of 10 mm outside diameter arranged in 12 rows in a staggered arrangement with a tower width of 0.6 m. Each row is 1.2 m in the horizontal direction. The longitudinal and transversal spacing of the tubes are 0.02 m and 0.06 m, respectively. Nominal operating conditions for the tower are: air flow rate m_a = 3.0 kg s^{-1}, cooling water flow rate m_c = 0.8 kg s^{-1}, spray water flow rate m_s = 1.37 kg s^{-1}, inlet cooling water temperature t_{c1} = 21°C, and inlet wet bulb temperature t_{wb1} = 16°C.

Measurements of the prototype tower operation with various operating conditions were carried out by the Faculty of Engineering - University of Porto (Facão and Oliveira, 1999). The test operating conditions were: $0.58 \le m_a \le 1.7$ kg s^{-1}, $0.4 \le m_c \le 0.8$ kg s^{-1}, $0.20 \le m_s \le 1.39$ kg s^{-1}, $15 \le t_{c1} \le 28$ °C, and $10 \le t_{wb1} \le 20$ °C. Measurement results are described in (Facão and Oliveira, 2000). They studied the effects of the operating parameters on the thermal efficiency of the tower ε defined as

$$\varepsilon = \frac{t_{c1} - t_{c2}}{t_{c1} - t_{wb1}} \tag{2.13}$$

Their observations were that: t_{c1} had a very little influence on ε, increase of m_s resulted in an increase in ε until complete wetting of the surfaces occurred at about 1 kg s^{-1} beyond that it made no significant improvement, and ε increased with the increase of m_a and decreased with the increase of m_c.

Model results

Data from the measurements are fed to the model as input data. To find the mass transfer coefficient K, the outlet cooling water temperature t_{c2} from the prototype tower measurements is taken as input to the model. The correlation equation for the mass transfer coefficient concluded from 60 sets of measurement data is

$$K = 0.065 G_a^{0.773} \qquad 0.96 < G_a \text{ (kg s}^{-1}\text{ m}^2\text{)} < 2.76 \tag{2.14}$$

where G_a is the air mass velocity at the minimum flow section between the tubes. This correlation is shown in Fig. 2.4 on a logarithmic scale, together with correlations from other works (Parker and Treybal, 1962; Mizushina et al. 1967; Niitsu et al., 1969). Figure 2.4 shows that Eq. (2.14) falls within the range of similar correlations.

Establishing the transfer coefficients, K from Eq. (2.14) and α_s from literature (e.g. Parker and Treybal, 1962), the model can be used to predict the performance of the tower with variable flow rates and outdoor air conditions. The prototype tower tests didn't include the tower operation at the nominal airflow of 3.0 kg s^{-1}. However, it is possible to predict the tower performance for this airflow rate. Figure 2.5 shows the predicted temperature and enthalpy distributions for the mid-row elements along the tower for the nominal conditions. Row number 1 refers to the lowest row in the tower.

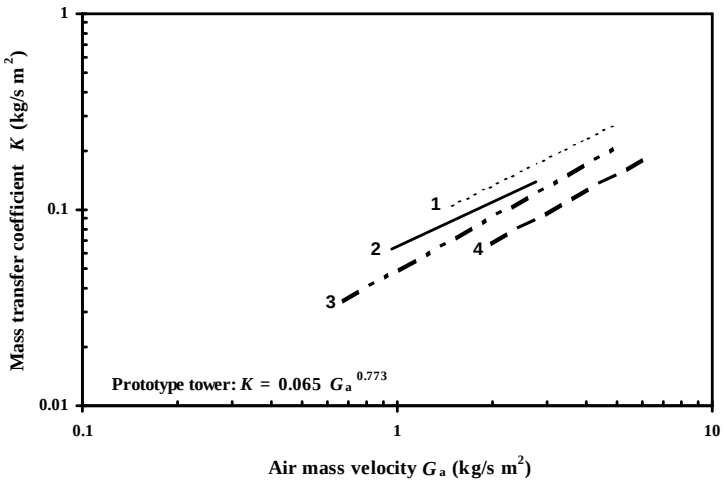

Fig. 2.4. Mass transfer coefficient from the experimental measurements: (1) Niitsu et al. (1969), (2) Prototype tower; (3) Parker and Treybal (1962), (4) Mizushina et al. (1967).

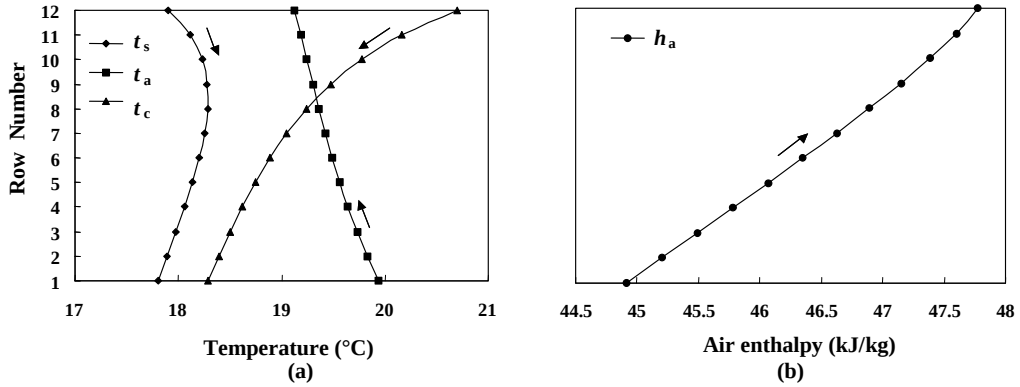

Fig. 2.5. Calculated temperature (a) and enthalpy (b) for the mid-row elements along the tower.

For the upper rows, and as a result of the relatively high cooling water temperature and air enthalpy, part of the heat lost by the cooling water is retained in the spray water, resulting in an increase of t_s. While for the lower rows, the spray water loses its heat to air at an increased rate due to the low air enthalpy, resulting in a decrease of t_s. This is shown by Fig. 2.5, which also shows a cooling water temperature decrease and air dry bulb temperature decrease along the corresponding flow paths (downwards for cooling water and upwards for air). The spray water is directly affected by the evaporative cooling, which makes it in a closer approach to the wet bulb temperature. The inlet air dry bulb temperature is taken to be 20°C, and as it appears from Fig. 2.5a, the air dry bulb temperature is higher than spray water temperature. Therefore the direction of sensible heat transfer is from air to spray water which results in a decrease of air dry bulb temperature. However, this behaviour depends on the value of the inlet air temperature. Although air is losing heat as sensible heat, the enthalpy of air is rising due to latent heat gain from the evaporation of spray water at the saturated air-water interface. The increase of air enthalpy is shown in Fig. 2.5b.

Optimisation of flow rates and number of tubes and rows

Model output shows that for the nominal tower operating conditions, the predicted rejected heat q_c is 9250 W and the coefficient of performance COP is 4.6. Based on the fan and pump measurements for other operating conditions, the estimated total power consumption for the nominal case is 1990 W, where the fan power is 1850 W. The COP is defined as

$$\mathrm{COP} = \frac{q_c}{W_{tot}} \tag{2.15}$$

where W_{tot} is the total power consumption for the cooling tower (sum of the fan power and the spray water pump power). For a specific geometry, the total power consumption W_{tot} is a function of the air velocity inside the tower. As the latter increases, the rejected heat q_c will increase, but the COP will decrease.

If the longitudinal and transversal tube spacing is kept similar to that of the prototype tower, a study of the optimum overall tower geometry (in terms of the number of tubes and rows) can be carried out. This can be achieved by considering the pressure drop data from the test measurements as a basis to estimate the pressure drop for various air and water flow rates. The cooling tower model can be implemented to estimate the tower thermal performance where the mass transfer coefficient is a function of the air velocity (Eq. (2.14)). Therefore, the tower performance can be found for variable air velocities, number of tubes, and number of rows.

The rejected heat increases with the increase of the contact area. Furthermore, the power consumption for a large tower with a low air velocity is lower compared to a small tower with a high air velocity. Therefore, it could be concluded that better COP is obtained when operating with low air velocity and a high contact area. Model output data for the COP and the rejected heat can be calculated for different values of number of tubes and number of rows, from which, an optimum selection of the tower geometry can be made. Performing such analysis with the nominal operating temperatures and cooling water flow rate, it could be concluded that when the number of tubes is 24 and the number of rows is 18, the rejected heat is 10 kW and the COP 11.4, for which: m_a = 2.23 kg s^{-1}, m_s = 1.73 kg s^{-1}, W_{tot} = 875 W, and fan power = 700 W.

Cooling System Simulation

The model developed for the CWCT is integrated into a global system performance simulation program, which also includes the transient building simulation model TRNSYS (1996), chilled ceiling model, night cooling strategy, system control, and models for other components.

By using a climatic-dependent cooling system, overheating for a few days in the year is to be expected. It could be minimised by methods of utilising stored cooling energy, which can be produced during the night. These methods include the storage of cooling energy in the building mass by implementing a night cooling strategy (Sprecher et al. 1995) or the storage of cooled water in suitable tanks.

An office building is considered for the simulation. Each room in the building has a floor area of 9.7 m^2, and there exists one occupant, and appliances (a computer, a printer, and lighting), which are used for 8 hours on working days. A medium value of 67.5% is taken for the ratio of the chilled ceiling area to the floor area. A simple night cooling control is adapted. The optimised number of tubes and rows are considered for the CWCT in the simulations. A criterion is applied that limits a total maximum annual of 40 hours for the room temperature higher than 26°C. The simulation is carried out using the climatic test reference year files for four European cities: Helsinki, Lisbon, London, and Zurich. The results of the simulation show that the yearly COPs are higher than those for systems using conventional vapour compression machines. As an example, for an office building in Zurich with a total floor area of 563 m^2, the simulation program shows an average system COP of 8.4 for the period April to October.

Later, a French paper by Bolher et al. (2002) shows results from a building simulation program for a cooling system using an open type cooling tower with chilled ceilings for several locations in France. A heat exchanger between the cooling tower water circuit and the chilled ceiling water circuit was considered. Their results indicate that such a technology has promising potential for low and medium loads when associated with an appropriate control strategy.

The utilisation of cooling towers in the cooling of buildings implies that the spray water temperature will be relatively low. This would mean minimum possibilities for the growth of the bacterium Legionella pneumophila. The optimum temperature for the bacterium growth is 37°C. Below this temperature, the multiplication rate decreases and is considered insignificant below 20°C (CIBSE, 2000).

Results from other tests

An office building in Urdorf (CH) was subjected to tests by Sulzer Infra Lab AG (CH) where a 300 m^2 area of chilled ceiling was connected to a CWCT. The measurements showed acceptable indoor air temperatures. Maximum recorded indoor temperature was 27°C in one room. An average system COP of 6.2 is reported for the period July-October (Sprecher et al. 2000; Oliveira et al. 2000).

Recently, an experimental research was carried out (Costelloe and Finn, 2003) for the energy performance of an open type cooling tower used to generate cooling water at temperature levels suitable for chilled ceiling applications. The test rig was located in Dublin, Ireland and included two circuits, a cooling water circuit and a chilled ceiling

circuit, where an intermediate heat exchanger existed between the two circuits. The results indicate that a COP value from 7.5 to 11.4 was achieved at the tower's full load, while at partial loads it was 5.4 to 8.1.

These test results support the conclusion reached by this thesis with respect to the feasibility of using cooling towers in conjunction with chilled ceilings in the cooling of buildings.

3 SIMPLIFICATION OF ANALYTICAL MODELS AND INCORPORATION WITH CFD FOR THE PERFORMANCE PREDICTION OF CLOSED WET COOLING TOWERS

The reviewed literature (Section 1.1) showed that different assumptions were considered in the analytical solution of CWCTs. One main assumption was the spray water temperature, which was considered as constant along the heat exchanger (Mizushina et al., 1967; Niitsu, 1969; Koschenz, 1995). However, the accuracy of the results with such assumptions was not quantified with respect to other approaches or relevant experimental measurements.

In addition to the analytical solution, computational fluid dynamics (CFD) has been implemented in the analysis of CWCTs. In this case, boundary conditions of heat flux distribution have to be defined. A constant heat flux in the tower was assumed (Gan and Riffat 1999) and a linear heat flux distribution along the tower was considered (Gan et al., 2001). The conclusion from these two works is that CFD could be used in the design of CWCTs when a proper distribution of heat flux is incorporated. The latter could be obtained from models of the thermal performance of the tower or experimental measurements.

In paper II, analytical models for cooling towers are simplified, compared to other models, and validated with respect to experimental results for the prototype CWCT. The analytical results for the heat distribution are then incorporated with CFD to predict the performance of the tower for different air flow patterns.

3.1 Simplification of analytical models

3.1.1 Simple models

3.1.1.1 Computational model results

The computational model, described in Chapter 2, gives the following results for the nominal operating conditions: total rejected heat is 9250 W, total sensible heat 2780 W, outlet cooling water temperature t_{c2} 18.23°C and inlet or outlet spray water temperature (t_{s1} or t_{s2}) 17.76 °C.

For the three fluids flowing inside the tower, the heat gain or loss per row for one tube is shown in Fig. 3.1. Row number 1 refers to the lowest row. For each row, the sum of the air heat and the spray water heat equals the cooling water heat. As it is shown, the distribution of the cooling water heat is not constant; it is higher for the upper rows due to a higher cooling water temperature. Spray water gains heat rapidly near the upper

rows. The air latent heat and sensible heat are in opposite directions and the difference between them represents the air enthalpy rise.

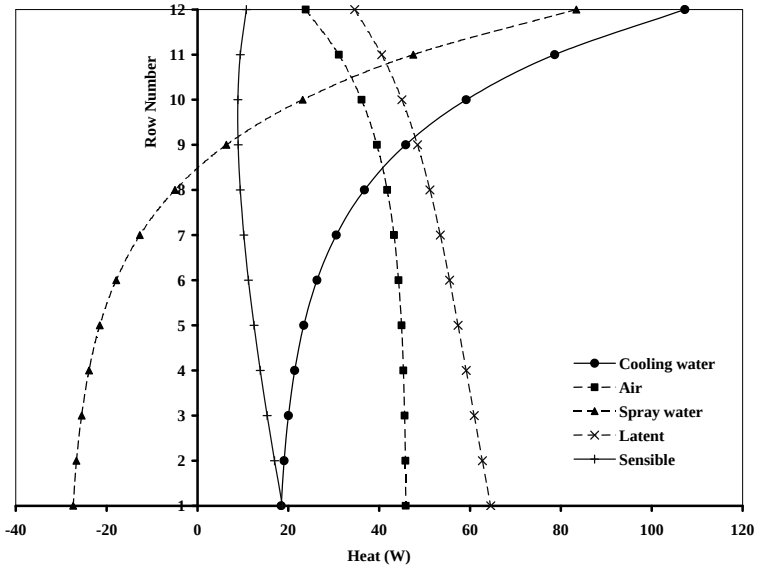

Fig. 3.1. Computational model output: heat distribution per row for one tube.

Spray water temperature

The computational model involves setting up arrangements for the exchanged data between the elements inside the tower due to the different flow directions of the fluids inside the elements. Applying proper assumptions for the spray water temperature inside the tower can lead to simple analytical approaches. For a one-dimensional uniform flow of air, two simple models can be presented: a constant spray water temperature $\overline{t}_s$, and an extension of this assumption to $\overline{t}_s = t_{c2}$.

Constant spray water temperature $\overline{t}_s$

Figure 2.5a shows that the variation of spray water temperature along the tower is small. Therefore, it could be assumed that the spray water temperature is constant and equal to $\overline{t}_s$.

First, the solution will be considered for the whole tower. The rate of heat transfer from the cooling water to the spray water, through the tube wall, is presented in Eq. (2.1). Integrating Eq. (2.1) from the inlet to the outlet of cooling water, with constant $\overline{t}_s$, gives

$$\frac{U_o A_t}{m_c C_w} = \ln\left(\frac{t_{c1} - \overline{t}_s}{t_{c2} - \overline{t}_s}\right) \tag{3.1}$$

where A_t is the total outside area of the tubes.

For the heat transfer between the saturated air-spray water interface and the air bulk, the whole process is based on the enthalpy difference according to the Merkel equation (Eq. (2.8)). Integrating Eq. (2.8) from the inlet to the outlet of air gives

$$\frac{K A_{\mathrm{t}}}{m_{\mathrm{a}}} = \ln\left(\frac{h'_{\mathrm{s}} - h_{\mathrm{a1}}}{h'_{\mathrm{s}} - h_{\mathrm{a2}}}\right) \tag{3.2}$$

Equations (3.1 and 3.2) comply with the log-mean definitions for temperature and enthalpy differences, respectively. The coefficients U_{o} and K in these equations are overall heat and mass transfer coefficients, respectively.

The energy balance for the fluids flowing in the tower gives

$$m_{\mathrm{c}} C_{\mathrm{w}} (t_{\mathrm{c1}} - t_{\mathrm{c2}}) = m_{\mathrm{a}} (h_{\mathrm{a2}} - h_{\mathrm{a1}}) \tag{3.3}$$

The tower inlet data are usually known: the mass flow rates (m_{a} and m_{c}), and the inlet operating conditions (t_{c1} and h_{a1}). Besides these, the transfer coefficients (K and U_{o}) should be defined. In the current analysis, α_{s} is evaluated according to the empirical correlation by Parker and Treybal (1962) and K is evaluated according to Eq. (2.14). Note that h'_{s} is the enthalpy of saturated air at the constant spray water temperature $\overline{t}_{\mathrm{s}}$. The tower outlet data (t_{c2} and h_{a2}) and the spray water temperature $\overline{t}_{\mathrm{s}}$ can be found by solving the three equations (3.1, 3.2, and 3.3) where iterations have to be implemented. No special assumption was made for the relation between the spray water temperature and enthalpy of the saturated air, as general psychrometric relations are applied for the thermal properties in the model.

Now to find the heat distribution along the tower: for any surface area of the tube A_{x} measured from the cooling water inlet uptower, the rejected heat from the cooling water is

$$q_x = m_{\mathrm{c}} C_{\mathrm{w}} (t_{\mathrm{c1}} - t_{\mathrm{c}}) \tag{3.4}$$

When Eq. (3.1) is applied for this surface area, A_{x} and t_{c} will appear in Eq. (3.1) instead of A_{t} and t_{c2}, respectively. Then, the substitution for t_{c} in Eq. (3.4) gives

$$q_x = m_{\mathrm{c}} C_{\mathrm{w}} (t_{\mathrm{c1}} - \overline{t}_{\mathrm{s}})(1 - \exp(-U_{\mathrm{o}} A_{\mathrm{x}} / m_{\mathrm{c}} C_{\mathrm{w}})) \tag{3.5}$$

The sensible heat transfer is

$$-m_{\mathrm{a}} C_{\mathrm{H}} \, \mathrm{d}t_{\mathrm{a}} = \alpha_{\mathrm{i}} (t_{\mathrm{a}} - \overline{t}_{\mathrm{s}}) \mathrm{d}A_{\mathrm{y}} \tag{3.6}$$

where A_y is the tube surface area measured from the cooling water outlet at the downtower. Implementing the Lewis relation ($\alpha_i / K\, C_H = 1$) and integrating from the air inlet section to any surface area A_y gives

$$\frac{K A_y}{m_a} = \ln\left(\frac{t_{a1} - \bar{t}_s}{t_a - \bar{t}_s}\right) \tag{3.7}$$

For which, the sensible heat transfer q_y is

$$q_y = m_a C_H (t_{a1} - t_a) \tag{3.8}$$

Substitution for t_a from Eq. (3.7) in Eq. (3.8) gives

$$q_y = m_a C_H (t_{a1} - \bar{t}_s)(1 - \exp(-K A_y / m_a)) \tag{3.9}$$

Eqs. (3.5 and 3.9) describe the distribution of the cooling water heat and the air sensible heat, respectively, along the tower.

Case where $\bar{t}_s = t_{c2}$

One further simplification of the model could be obtained by assuming that the constant spray water temperature $\bar{t}_s$ and the outlet cooling water temperature t_{c2} are equal. This assumption was suggested by Koschenz (1995). The analysis for the heat distribution will be similar to that presented above for $\bar{t}_s$. The concluded equations for the cooling water heat and the air sensible heat for this case will be, respectively, similar to Eqs. (3.5 and 3.9), except that $\bar{t}_s$ is replaced by t_{c2}.

$$q_x = m_c C_w (t_{c1} - t_{c2})(1 - \exp(-U_o A_x / m_c C_w)) \tag{3.10}$$

$$q_y = m_a C_H (t_{a1} - t_{c2})(1 - \exp(-K A_y / m_a)) \tag{3.11}$$

3.1.2 Results of the simplified models

The concluded equations describing the distribution of the cooling water heat and air sensible heat (Eqs. (3.5) and (3.9)) are simple equations in terms of the tower geometry and the operating conditions. This means that the heat distribution need not be assumed arbitrarily. The results obtained from the constant spray water temperature (constant $\bar{t}_s$)

model for the nominal tower data give: t_{c2} = 18.28°C, $\bar{t}_s$ = 18.07°C, the total rejected heat is 9090 W, and the total sensible heat 2830 W. These data agree well with those obtained from the computational model. Table 3.1 shows a comparison of a sample of the results, for the outlet cooling water temperature and the spray water temperature, from the simple analytical model (constant $\bar{t}_s$) with that from the experimental measurements. The data in the table cover the tested range of air volumetric flow rate (0.48, 1.08, and 1.36 $m^3\ s^{-1}$) and cooling water mass flow rate (0.40, 0.60, and 0.80 kg s^{-1}). It can be seen that the calculated and measurement results are in good agreement.

Table 3.1. Comparison between the experimental measurements and the results obtained from the simple analytical model with constant $\bar{t}_s$.

Supply air			Cooling water					Spray water		
V_a	t_a	RH	m_c	t_{c1}	$t_{c2(ex)}$	t_{c2}	$\frac{\Delta t_c}{\Delta t_{c(ex)}}$	m_s	$t_{s(ex)}$	t_s
$m^3\ s^{-1}$	°C	%	kg s^{-1}	°C	°C	°C	%	kg s^{-1}	°C	°C
0.48	16.07	50	0.40	18.54	15.67	15.74	98	1.37	15.10	15.67
0.48	21.33	43	0.60	21.18	19.15	19.06	104	1.38	18.56	18.97
0.48	13.08	84	0.80	18.53	17.02	17.03	99	1.38	16.47	16.90
1.08	26.19	47	0.40	23.96	20.82	20.71	104	1.37	20.37	20.66
1.08	19.71	46	0.60	18.01	15.89	15.89	100	1.38	15.33	15.80
1.08	13.03	87	0.80	15.86	14.35	14.48	91	1.38	13.85	14.36
1.36	19.74	43	0.40	17.77	14.78	14.83	98	1.38	14.30	14.77
1.36	32.50	30	0.60	23.86	21.84	21.70	107	1.37	21.43	21.61
1.36	16.21	94	0.80	18.99	17.39	17.58	88	1.38	16.79	17.46

V_a is the air volumetric flow rate, RH is the air relative humidity, $t_{c2(ex)}$ and $t_{s(ex)}$ are the experimental measurement for the outlet cooling water temperature and the spray water temperature respectively, and $\Delta t_c = t_{c1} - t_{c2}$.

For the case where $\bar{t}_s$ is assumed to equal t_{c2}, the solution suggests that: t_{c2} is 18.16 °C, total heat removal 9490 W and the total air sensible heat 2700 W. These results are also close to that from the constant $\bar{t}_s$ model. It is noticed that the ratio of the total sensible heat to the total cooling water heat is about 30% for the three methods (computational model, constant spray water temperature $\bar{t}_s$ and the assumption of $\bar{t}_s = t_{c2}$).

The results from the two simplified models show a maximum deviation of about 3%, for the total cooling water heat or the total air sensible heat, compared with that from the computational model. The discrepancies could be considered insignificant compared to the benefit gained from the simplification made in the solution. This reveals that simplified models could be used to assess the performance of CWCTs.

Figure 3.2 shows the distribution of the cooling water heat and the air sensible heat per row for one tube. The distribution for the three methods appears to be quite close. It can

be seen from Fig. 3.2 that the higher rows of the tower heat exchanger transfer more power than the lower ones. As more rows are added downtower, the heat rejected per row will decrease. This is a feature of a counter-flow heat exchanger. The higher rejected heat for the upper rows is due to the higher water temperature inside the tubes. From this it could be concluded that, to achieve a higher rate of cooling power, the height of the heat exchanger should be small and the surface area per a horizontal row of tubes should be large.

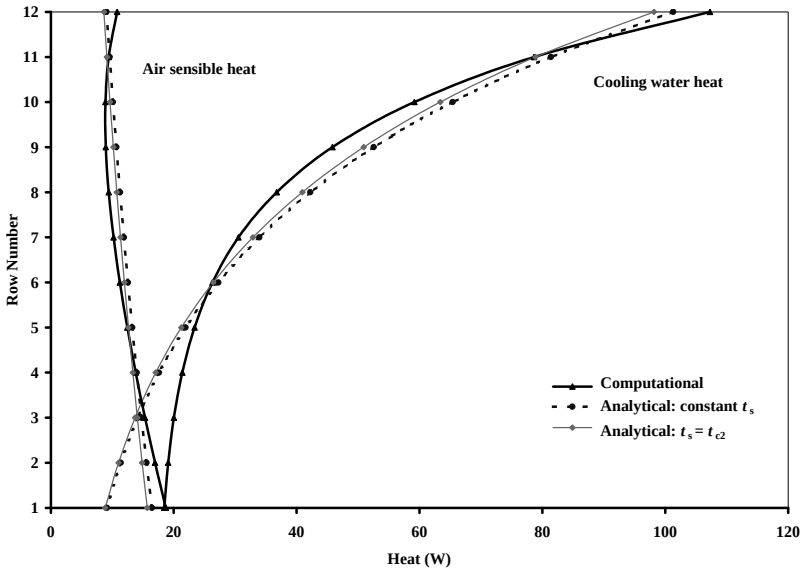

Fig. 3.2. Distribution of cooling water heat and air sensible heat along the tower per row for one tube calculated by the three methods.

3.2 Computational fluid dynamics (CFD) simulation

3.2.1 CFD model

The analytical solution of heat transfer in the cooling tower is here incorporated with CFD for the simulation of the general fluid flow and the performance of the prototype closed wet cooling tower.

A commercial CFD software package FLUENT (1995) is employed to predict the fluid flow in the cooling tower. The software solves multiphase fluid flow problems in a three-dimensional body-fitted coordinate system. The model for air flow consists of the conservation equations for mass, momentum, thermal energy and turbulence. A non-uniform computational grid of 119 x 259 is used for the simulation of the two-dimensional flow in the tower.

Assumptions

Tower configuration

A two-dimensional flow is assumed. The tower was designed such that outdoor air was supplied from one side wall. A total of nine flat baffles of different lengths are modelled and distributed uniformly between the fan outlet and the heat exchanger. This will improve the uniformity of fluid flow in the tower, so that the fluid flow above the baffles would be roughly symmetrical.

Heat exchanger

On a cross-section of a cooling tower for two-dimensional simulation, the tubes representing the heat exchanger become separate entities. Each tube is modelled as a smooth circular solid cylinder using the body-fitted coordinate system. The available software could not deal with the effect of evaporative cooling. Therefore, only the sensible heat transfer is considered which amounts to about 30% of the total cooling water heat. The sensible heat distribution is taken according to Eq. (3.9). The total heat transfer rate will be determined from its relation to the total sensible heat.

Spray water

The spray water is assumed to be composed of 100 trajectories of droplets in the two-dimensional flow. The mean diameter of the water droplets is 1.5 mm. The spray water is assumed injected into the tower through one nozzle at the centre line above the heat exchanger.

3.2.2 Results of fluid flow and thermal performance

Figure 3.3 shows the predicted air flow distribution inside the tower. The velocity vectors are plotted for every one in four grid lines along the width direction. It can be observed that the supply air flows from the left side wall below the heat exchanger and then flows upwards through the heat exchanger guided by the baffles. It appears that because of the bypass flow near the left side wall and the air recirculation between the baffles, the flow of air through the heat exchanger is not as uniform as expected. The effect can be seen from the direction of the velocity vectors in the enlarged graph in Fig. 3.3 especially for the lower rows. This could decrease the rate of heat transfer between air and tubes.

The thermal performance is predicted for the nominal operating conditions. The results indicate that the difference in the cooling water temperature between the top and bottom tube rows is 0.47 K. From which, the calculated sensible heat transfer between air and

tubes is 1564 W. This is much lower than the analytical result (2830 W), which could be attributed to the non-uniform distribution of air flow in the tower.

To investigate the effect of air flow distribution on the heat transfer, another prediction is carried out for air supply from the bottom of the tower, Fig. 3.4. In this case, the air flow through the heat exchanger appears to be very uniform. The predicted cooling water temperature difference across the heat exchanger increases to 0.81 K corresponding to a sensible heat transfer of 2710 W, which is close to the analytical solution. Therefore, the estimated total cooling water heat removal is 9030 W, which is close to the analytical solution.

These predictions show the importance of the air flow distribution on the thermal performance of a cooling tower. It is demonstrated that CFD can be used as a valuable tool for the design of cooling towers.

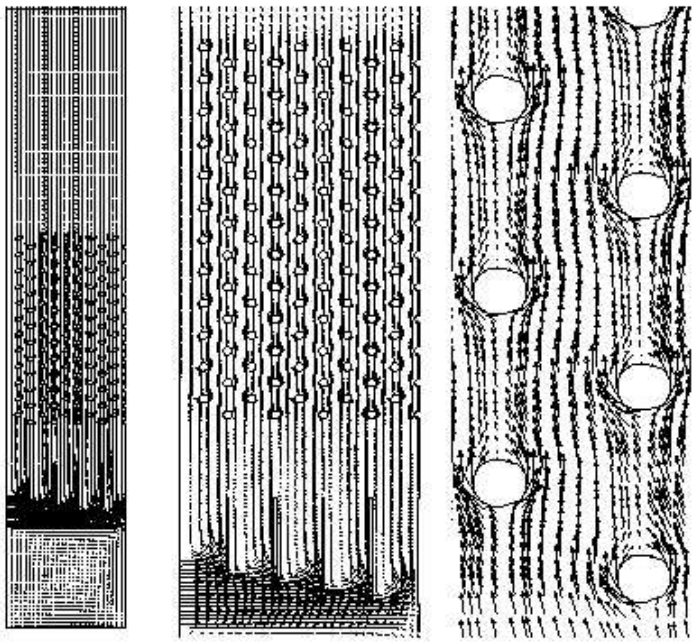

Fig. 3.3. Predicted air flow in half of the cooling tower with air supply from the left side wall.

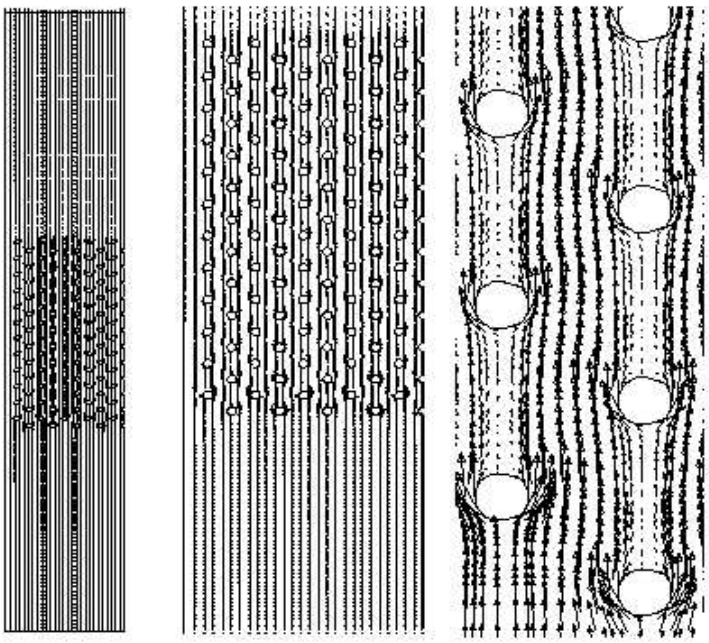

Fig. 3.4. Predicted air flow in half of the cooling tower with air supply from the bottom.

4 PERFORMANCE INVESTIGATION OF EVAPORATIVELY COOLED HEAT EXCHANGERS

4.1 Plain and Finned circular Tubes

Closed wet cooling towers (CWCTs), evaporative fluid coolers and evaporative condensers are examples of evaporatively cooled heat exchangers (ECHEs). The interest here is to investigate plain and finned tube cores in an ECHE and study the heat transfer characteristics and the energy efficiency of the process.

In this concern, Niitsu et al. (1969) performed experimental work on plain tubes in evaporative liquid coolers where the tubes were staggered 16 mm o. d. Besides they tested the tubes with circular fins of 42.6 mm diameter with two fin spacings (6.1 mm and 11 mm). Their conclusion was that the finned bank had much lower heat and mass transfer coefficients compared to the plain bank. This was attributed to possible water hold up between the fins and the low fin efficiency for the wet fins (Finlay and Harris, 1984). To the disputant's knowledge, only Niitsu et al. (1969) presented a comparison of the performance of plain circular and finned tubes.

The objective of the work presented by Paper III is to empirically compare the thermal and hydraulic characteristics of plain and plate-finned tubes in an ECHE.

4.1.1 Theoretical background

Fig. 4.1a shows a typical arrangement of an ECHE.

Plain tubes

The assumption of constant spray water temperature ($\overline{t}_s$) discussed in Section 3.1 will be considered in the current analysis. The relevant heat transfer equations (3.1, 3.2, and 3.3) will apply. Since water flowing inside the tubes is here defined as hot water, then the notation for cooling water t_c will be replaced by hot water t_h in those equations, the inlet and outlet hot water temperatures are t_{h1} and t_{h2}, respectively.

The expected trends of temperature and enthalpy distributions inside the heat exchanger, according to the analysis presented in the preceding chapters, are shown in Fig. 4.1b. In the present work, the constant spray water temperature $\overline{t}_s$ will be taken equal to the inlet spray water temperature t_{s1} measured from the experiments. This assumption seems acceptable according to the sketch of Fig. 4.1b.

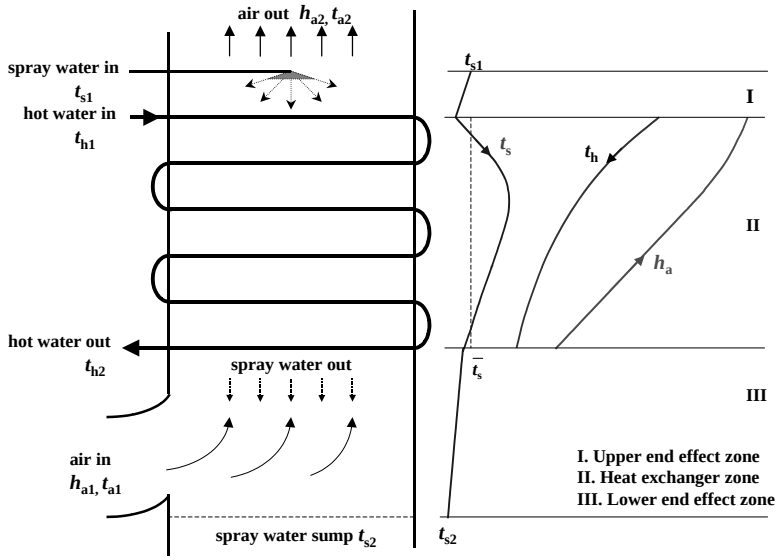

(a) (b)

Fig. 4.1. (a) Schematic of the evaporatively cooled heat exchanger (b) Expected temperature and enthalpy distribution along the exchanger.

Plate finned tubes

The spray water temperature along the heat exchanger (on the fin surface and the bare tube between the fins) will be considered constant and will be taken equal to the measured inlet spray water temperature t_{s1}, as was the case for the plain tubes. By considering an element including a fin as shown in Fig. 4.2a, the heat transfer from the hot water to air via the spray water film will be studied.

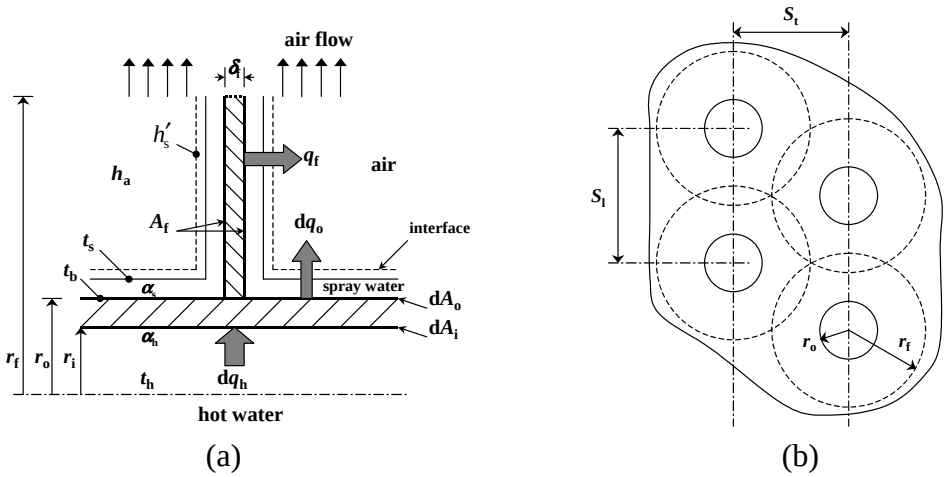

(a) (b)

Fig. 4.2. (a) Element in a finned tube (b) Approximation of a plate-fin by circular fins.

Heat transfer from the hot water to the spray water

For the element shown, the heat from the hot water inside the tube $\mathrm{d}q_\mathrm{h}$ flows to the spray water on the tube and fin outer surfaces. Combining this with the definition of the fin efficiency η_f, the following equation can be written

$$\mathrm{d}q_\mathrm{h} = \frac{t_\mathrm{h} - \bar{t}_\mathrm{s}}{\dfrac{1}{\alpha_\mathrm{s}}\left(\dfrac{1}{\eta_\mathrm{f} A_\mathrm{f} + \mathrm{d}A_\mathrm{o}}\right) + \dfrac{1}{\mathrm{d}A_\mathrm{i}}\left[\dfrac{1}{\alpha_\mathrm{h}} + \dfrac{r_\mathrm{i}}{k_\mathrm{w}}\ln\left(\dfrac{r_\mathrm{o}}{r_\mathrm{i}}\right)\right]} = -m_\mathrm{h} C_\mathrm{w}\,\mathrm{d}t_\mathrm{h} \tag{4.1}$$

Integrating Eq. (4.1) from the inlet to the outlet of the heat exchanger yields Eq. (3.1), in which $U_\mathrm{o} A_\mathrm{t}$ for the finned heat exchanger is defined as

$$\frac{1}{U_\mathrm{o} A_\mathrm{t}} = \frac{1}{\alpha_\mathrm{s}}\left(\frac{1}{\eta_\mathrm{f} A_\mathrm{ft} + A_\mathrm{ot}}\right) + \frac{1}{A_\mathrm{it}}\left[\frac{1}{\alpha_\mathrm{h}} + \frac{r_\mathrm{i}}{k_\mathrm{w}}\ln\left(\frac{r_\mathrm{o}}{r_\mathrm{i}}\right)\right] \tag{4.2}$$

where the heat transfer areas in this equation are the total for the heat exchanger: A_ft is the total finned area, A_ot is the total outer surface area of the bare tubes between the fins, and A_it is the total inner area of the tubes.

The plate fin is approximated by circular fins of radius r_f (Fig. 4.2b) having equivalent performance (Threlkeld, 1970)

$$r_\mathrm{f} = \sqrt{\frac{S_\mathrm{l} S_\mathrm{t}}{\pi}} \tag{4.3}$$

where S_l and S_t are the longitudinal and transversal tube spacing, respectively. For heat transfer from a circular fin of uniform thickness δ_f and fin thermal conductivity k_f to the surroundings at temperature $\bar{t}_\mathrm{s}$, the simple approximate formula by Schmidt (1949) gives

$$\eta_\mathrm{f} = \frac{\tanh(M r_\mathrm{o} \phi)}{M r_\mathrm{o} \phi} \tag{4.4}$$

where $M = \sqrt{\dfrac{2\alpha_\mathrm{s}}{k_\mathrm{f}\delta_\mathrm{f}}}$, $\phi = \left(\dfrac{r_\mathrm{f}}{r_\mathrm{o}} - 1\right)\left[1 + 0.35\ln\left(\dfrac{r_\mathrm{f}}{r_\mathrm{o}}\right)\right]$

r_f, r_o and r_i are the fin and tube radiuses as defined by Fig. 4.2.

Heat transfer from the spray water to the moist air

Heat transfer takes place from the spray water film to the moist air through the air-spray water interface. The latter could be assumed saturated at the spray water temperature $\bar{t}_s$. Heat transfer consists of sensible heat and latent heat due to mass transfer. Equation (3.2) can be implemented to calculate the heat transfer from the interface to the air stream, where A_t will refer to the total wet surface area of the fins and tubes (sum of A_{ft} and A_{ot}).

Equation (3.3) can be implemented between the heat exchanger inlet and outlet for the total heat balance of the fluids flowing inside the heat exchanger.

When the geometry of the heat exchanger and the transfer coefficients (α_s, α_h, K) are specified and the inlet operating conditions (m_h, m_a, t_{h1}, h_{a1}) are taken as input, the outlet conditions (t_{h2}, h_{a2}, and $\bar{t}_s$) can be found by solving, by iterations, the equations corresponding to Eqs. (3.1, 3.2, and 3.3).

4.1.2 Experimental work

Figure 4.3 shows a schematic diagram of the experimental test system. The system included flow of three fluids (air, hot water, and spray water). An electric heater provided the load in the hot water circuit. Two pumps were used, one for the hot water, and the other one for the spray water. Spray water was injected onto the surfaces of the heat exchanger by a spray nozzle. Air was introduced to the heat exchanger by means of a fan.

The tubes are circular copper tubes arranged in a staggered equilateral pitch of 2.8D in eight rows. The number of tubes is four. Tube o. d. is 10 mm. The fins are copper plates. The number of plate-fins is six, each of 0.5 mm thickness. Fin spacing is 12 mm, which is considered to ease spray water flow along the fins. The plain tube and finned tube heat exchangers occupy the same volume. The ratio of total contact area (finned tubes/plain tubes) is four.

Three airflow rates were considered: 0.0151, 0.0235, and 0.0323 kg s^{-1}, which correspond to air velocities in the minimum flow area of 1.58, 2.45, 3.4 m s^{-1} for the plain tubes, and 1.66, 2.57, 3.57 m s^{-1} for the finned tubes. The hot water flow rate was constant during the experiments. Three nominal inlet hot water temperatures t_{h1} (30, 32 and 34 °C) were considered.

The spray water flow rate for the plain tubes was 0.025 l s^{-1} (90 l hr^{-1}), which was increased to 0.055 l s^{-1} (200 l hr^{-1}) for the finned tubes to ensure wetting of all of the exposed surfaces.

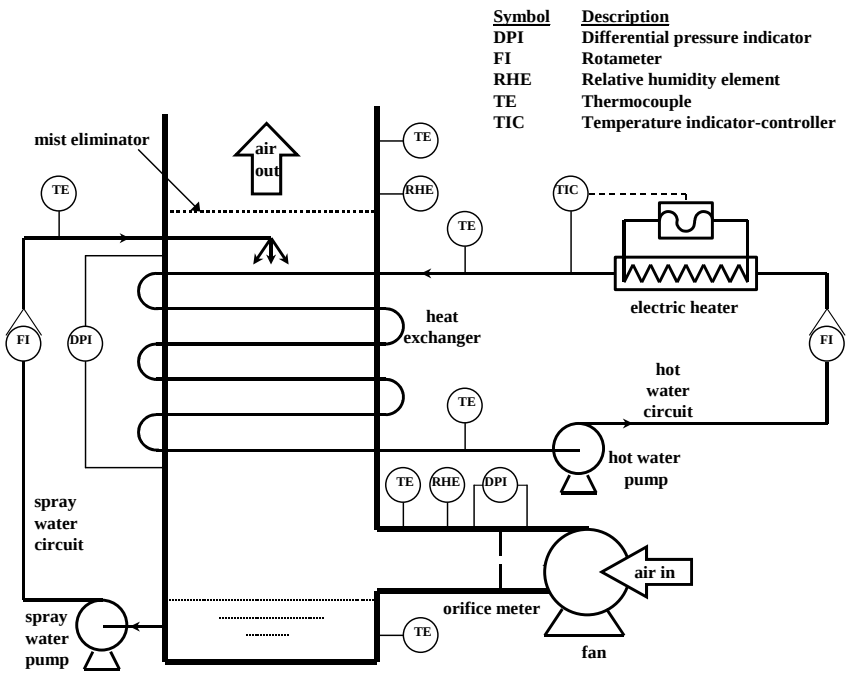

Fig. 4.3. Schematic diagram of the experimental test system.

4.1.3 Results and discussion

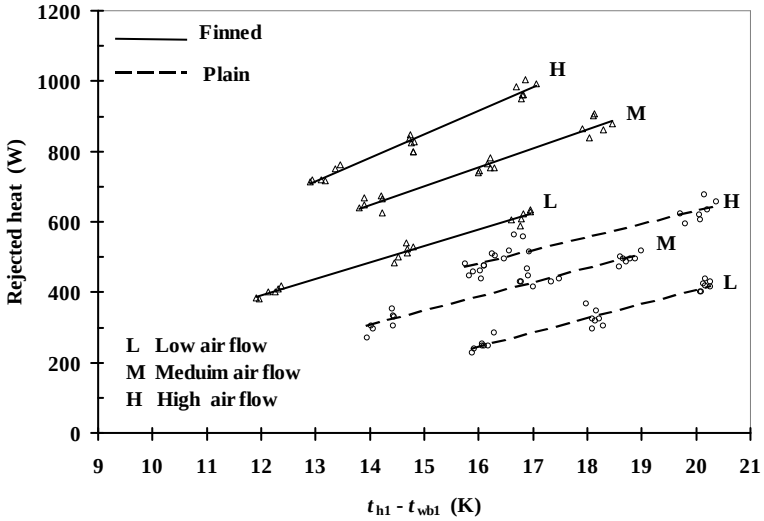

Fig. 4.4. Measured thermal performance of the plain and finned tubes.

The thermal performance of the plain and finned tubes is shown in terms of the rejected heat in Fig. 4.4. The horizontal axis represents the difference between the inlet hot water temperature t_{h1} and the outdoor air wet-bulb temperature t_{wb1}, which could be considered as a measure of the temperature-difference potential available at the inlet. For a specific tube geometry (plain or finned), the influence of higher airflow rate or higher temperature-difference potential is higher rejected heat. Major improvements in

heat transfer take place when using the plate-finned tubes. For example, for $t_{h1} - t_{wb} = 16$ K, the ratio of heat transfer (finned to plain) ranges from 1.92 to 2.40 for the implemented airflow rates.

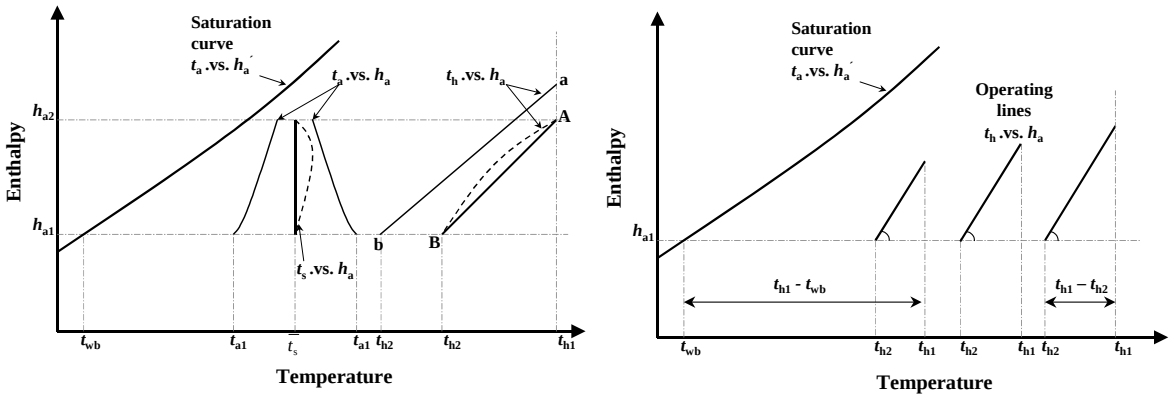

Fig. 4.5. Temperature-enthalpy diagram for an ECHE.

The dashed curves in Fig. 4.5a show the actual relation between the hot water temperature and the air enthalpy (t_h .vs. h_a) and the spray water temperature and the air enthalpy (t_s .vs. h_a). For the assumption of constant spray water temperature ($\bar{t}_s$), Eq. (3.3) shows the thermal balance for the flow streams inside the cooler. From which, the following equation can be written

$$\frac{h_{a2} - h_{a1}}{t_{h1} - t_{h2}} = \frac{m_h C_w}{m_a} \tag{4.5}$$

This equation implies that the relation between the inlet and outlet operating points is linear. This is drawn on Fig. 4.5a. by the operating line A-B, which has a slope equal to (m_h C_w / m_a). For a constant hot water flow rate m_h, the effect of a higher air flow rate m_a is a lower slope for the operating line according to Eq. (4.5). Line a-b in Fig. 4.5a shows this case for the constant inlet hot water temperature t_{h1} and air inlet enthalpy h_{a1}, which will produce a lower outlet temperature t_{h2} and, consequently, more rejected heat. This case was also shown in Fig. 4.4 from the measurement results.

The air temperature inside the ECHE could increase or decrease, depending on the inlet air dry bulb temperature t_{a1} and the spray water temperature $\bar{t}_s$. The latter in turn depends on the level of the hot water temperature inside the tubes. This is shown by the two curves for (t_a .vs. h_a) in Fig. 4.5a.

Figure 4.5b shows an example of the operating lines for three inlet hot water temperatures t_{h1} under constant inlet operating conditions similar to three cases experimentally tested with constant flow rates (m_h and m_a). The slope is the same for the

three lines. When t_{h1} decreases, the temperature difference potential available at the inlet ($t_{h1} - t_{wb}$) decreases too, which results in lower rejected heat ($t_{h1} - t_{h2}$), as may be seen from Fig 4.4. This is also demonstrated in Fig 4.5b.

The model can calculate α_s and K when measurements data at the heat exchanger outlet are fed as input data. Figure 4.6 shows α_s from the measurement data. A scatter of values of α_s can be seen in this figure. Such a scatter of α_s can also be noticed in data indicated by Mizushina et al. (1967) and Dreyer and Erens (1990). The average value of α_s from the measurements for the finned tubes is 2268 W m^{-2} K^{-1}, and for the plain tubes is 1898 W m^{-2} K^{-1}. From our observations of the spray water flow inside the test section, no water hold up between the fins was noticed. For plain circular tubes and for spray water loading Γ/D = 1.78 kg s^{-1} m^{-2}, the value of α_s (W m^{-2} K^{-1}) is: 2544 (Mizushina et al., 1967), 1696 (Parker and Treybal, 1962), and 1290 (Niitsu et al., 1969). For finned tubes, the last mentioned authors indicated a correlation that gives α_s = 744 W m^{-2} K^{-1}, while for finned in-line tube evaporative condensers, Leidenfrost and Korenic (1986) indicated that α_s = 2920 W m^{-2} K^{-1}.

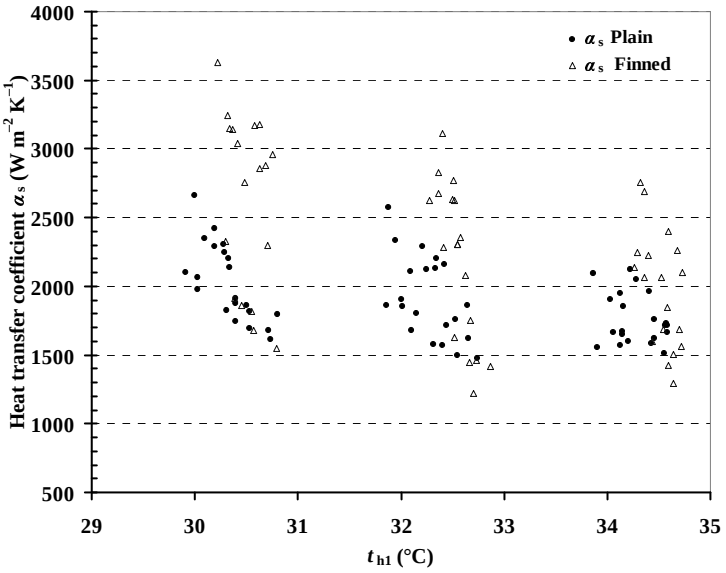

Fig. 4.6. Heat transfer coefficient α_s for the plain and finned tubes from the measurement data.

The average fin efficiency η_f found from this work is 43%. Wet fins have low efficiencies when compared to dry fins (Niitsu, 1969; Kried et al., 1978; and Erens, 1988). This is due to a relatively high heat transfer coefficient between the fin surface and the water film (α_s). The utilisation of wet extended surfaces will increase the total mass transfer from the spray water, which will increase the amount of heat transfer from the hot water despite the fact that the fin efficiency could be low.

Figure 4.7 shows the mass transfer coefficients K (kg s^{-1} m^{-2}) for the plain and finned tubes of the current work. The plain tubes have higher K values. However, the ratio of

total contact area (finned tubes/plain tubes) is four, which results in higher heat transfer rates for the finned tubes.

The K values for the current work are correlated as: $K = 0.077\ v_{max}^{0.812}$ for the plain tubes, and $K = 0.054\ v_{max}^{0.874}$ for the finned tubes, where v_{max} is the air velocity (m s^{-1}) at the minimum section.

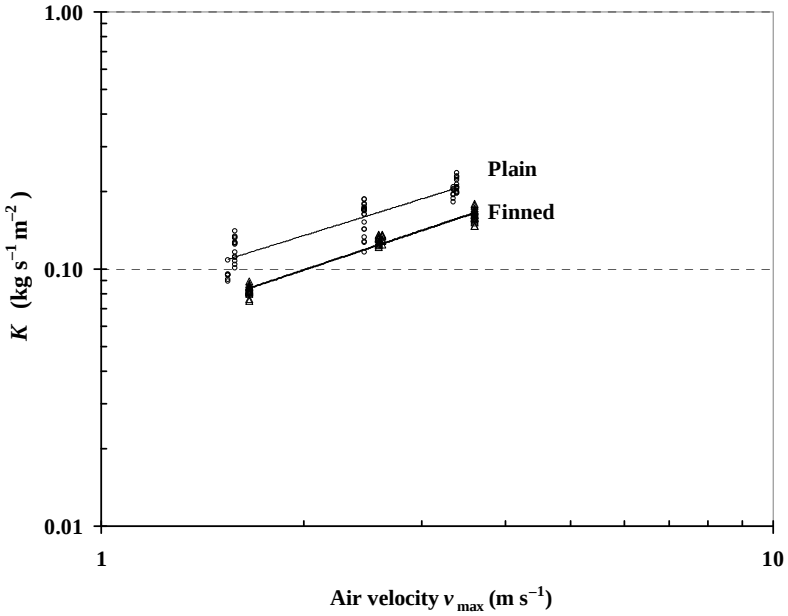

Fig. 4.7. Mass transfer coefficient K for the plain and finned tubes from the measurement data.

The relative thermal-hydraulic characteristic is expressed by an energy index (E). It is defined as the ratio of the volumetric thermal conductance ($U_o\ A_t\ /\ V$) to the air pressure drop per unit length ($\Delta p\ /\ z$):

$$E = \frac{U_o A_t}{V} \Big/ \frac{\Delta p}{z} \tag{4.6}$$

V is the volume ($V = A_{cs}\ z$, where A_{cs} is the cross sectional area). The thermal conductance is: $U_o\ A_t = q/\ (\Delta t_h)_{lm}$, where $(\Delta t_h)_{lm}$ is the log-mean temperature difference. Since $q = m_h\ C_w\ (t_{h1} - t_{h2})$, then E can be rewritten as

$$E = \frac{m_h C_w}{A_{cs} \Delta p} \ln\left(\frac{t_{h1} - \overline{t_s}}{t_{h2} - \overline{t_s}} \right) \tag{4.7}$$

The energy index E is shown in Fig. 4.8 versus v_{max}, the air velocity in the minimum cross section between the tubes. It appears from this figure that the plain tubes and the

finned tubes have close energy indices. This means that for a specific volume, the finned tubes transfer higher rates of heat with the same energy index. These results are indicative of favourable features for evaporative finned surfaces which need to be further studied, in terms of fin geometry and air and spray water flow rates, for better performance.

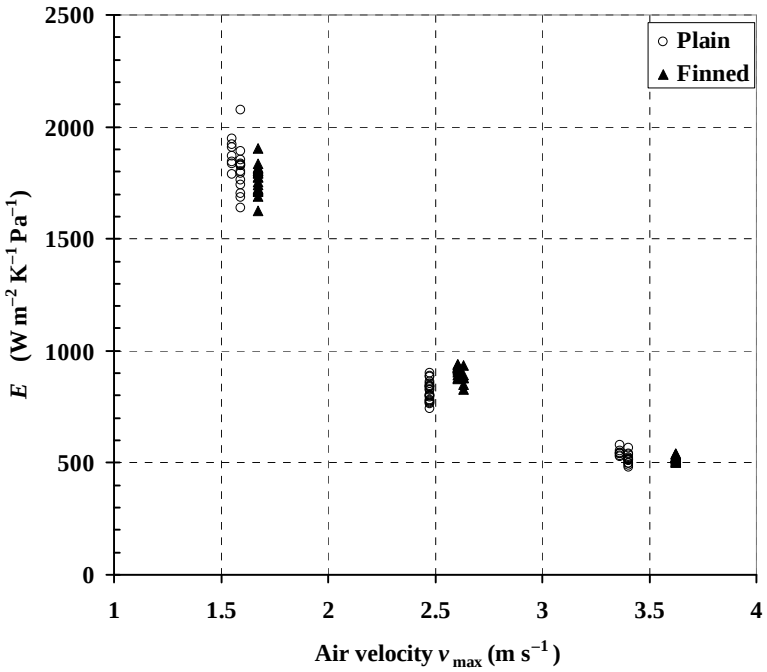

Fig. 4.8. Energy index for the plain and finned tube heat exchangers.

Fin material of construction

Results from a numerical analysis by Erens (1988) for an evaporative liquid cooler with the tubes placed integrally in a fill indicate that the fins can also be made with a nonconducting material, such as PVC. Despite the fact that plastic is a bad heat conductive material, fins as extended surfaces provide a larger area for mass transfer, which results in a lowering of the spray water temperature. This improves the amount of heat transfer from the tubes, which occurs through the direct contact of the spray water on the tube wall. A main advantage of a plastic wet surface is that it is corrosion resistant. However, attaching plastic fins to metallic tubes presents a practical difficulty. A suggestion could be made that plastic wet surfaces be added separately as packing, which could be placed above or under the heat exchanger coil. However, this does not mean that plastic tubes should be used.

4.2 Plain circular and oval tubes

If a heat exchanger is constructed from oval tubes (where the major axis is parallel to air flow), the expected pressure drop of the air flow will be low. This will lower the pumping power required by the fan, which is the main source of energy consumption in an air cooled heat exchanger. In addition, oval tubes can increase the compactness of heat exchangers as more tubes can fit into a specified volume. To the best knowledge of the disputant, there has not been published any paper in the open literature studying the utilisation of oval tubes in evaporatively cooled heat exchangers.

The objective of Paper IV is to compare, experimentally, the thermal and hydraulic performance of plain circular and oval tubes in ECHEs. The work is a continuation of the work of Paper III under similar operating conditions so that differences in performance will be as a result of the change in the tube shape to oval.

4.2.1 Experimental work

The test rig is the same one that was used to test the circular plain and finned tubes mentioned in 4.1.2.

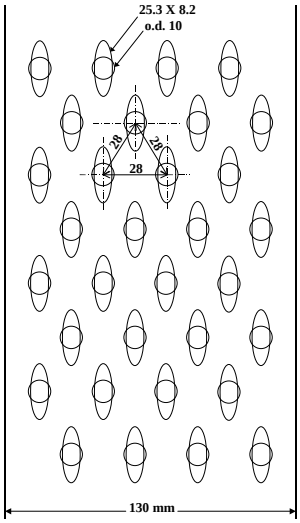

Fig. 4.10. The distribution of the circular and oval tubes in the test section.

There are four oval tubes per row; the total number of rows is eight. The tubes are arranged in a staggered configuration. The centres of the oval tubes coincide at the centres of the circular tubes investigated in Section 4.1 and as shown in Fig. 4.10. The oval tube was formed by heating and then pressing a circular copper tube in a proper mould. For manufacturing reasons, circular tubes having 18 mm o. d. were pressed into oval tubes. The circular tubes in Section 4.1 had 10 mm o. d. The formed oval tubes have a major axis of 25.3 mm and a minor axis of 8.2 mm. The axis ratio (major axis / minor axis) is 3.085. The perimeter of the oval tube is equal to the perimeter of the

circular tube from which it was formed. The tests were conducted under operating conditions similar to those for the circular tubes in Section 4.1 (air and hot water flow rates and nominal inlet hot water temperatures). The three air velocities in the minimum flow area were 1.47, 2.29, 3.15 m s^{-1}. The spray water flow rate for the oval tubes was 0.0375 l s^{-1} (135 l hr^{-1}). This flow rate was sufficient to wet the external surfaces of the tubes.

4.2.2 Results and discussion

To include the effect of the difference in the surface area for the oval and circular tubes, the heat flux can be considered. The characteristic length D_o for the oval tube is taken equal to the outside diameter of a circular tube which has an equivalent perimeter (here D_o = 18 mm). This is in accordance with a definition made by Ota et al. (1984). Furthermore, the effect of the outdoor wet bulb temperature t_{wb1} could be considered by taking the temperature-difference potential at the inlet (t_{h1}– t_{wb1}). A thermal performance parameter θ is defined as

$$\theta = \frac{t_{h1} - t_{h2}}{(t_{h1} - t_{wb1})\, D_o} \tag{4.9}$$

Noting that the hot water flow rate was constant during the experimental tests so that (t_{h1}– t_{h2}) refers to the rate of heat transfer, and that the lengths of the tubes were equal, then (t_{h1}– t_{h2}) D_o^{-1} refers to the heat flux (heat transfer per surface area). The parameter θ is shown in Fig. 4.11 versus v_{max}, the air velocity in the minimum flow area between the tubes. It appears from Fig. 4.11 that θ is lower for the oval tubes (on average it is 79% of that for the circular tube). The reason could be the larger frontal area of the circular tube and the related higher turbulence induced on its backside which may also affect the next tube in the tube bank resulting in higher rate of heat and mass transfer from the surfaces.

The same assumptions for the theoretical analysis of the plain tubes mentioned in Section 4.1 are implemented here (constant spray water temperature $\overline{t_s}$, which is equal to the measured inlet spray water temperature t_{s1}). The heat transfer coefficient between the tube surface and the spray water α_s is presented in Fig. 4.12. Values of α_s for the oval tubes in Fig. 4.12 extend over that for the circular tubes (the average is 12 % higher).

For the investigated oval and circular tubes, the hot water flow area inside the oval tube is 1.86 times the circular tube area. So, for the constant hot water flow rate, this means a corresponding lower hot water velocity. When the Gnielinski correlation (Incropera and DeWitt, 1996) is implemented to estimate the heat transfer coefficient inside the tube, it shows that α_h decreases by about 50% for the oval tube. The heat transfer rate from the hot water to the spray water is dependant on both α_s and α_h. Noting that α_s and α_h are of

the same order of magnitude, the final effect will be a decrease in the heat flux for the oval tube.

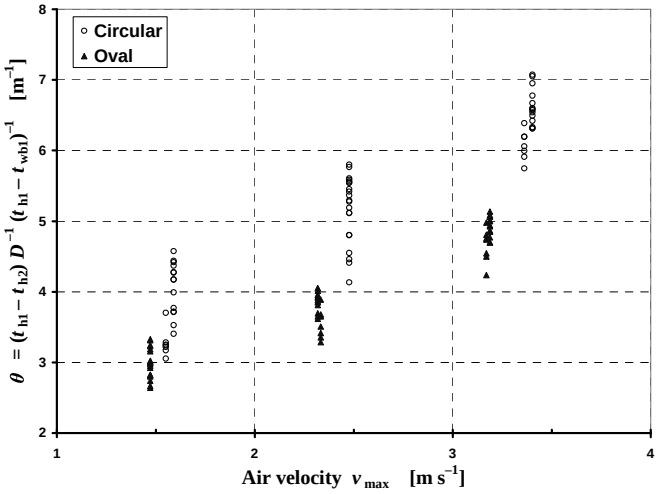

Fig. 4.11. Thermal performance parameter θ for the circular and oval tubes.

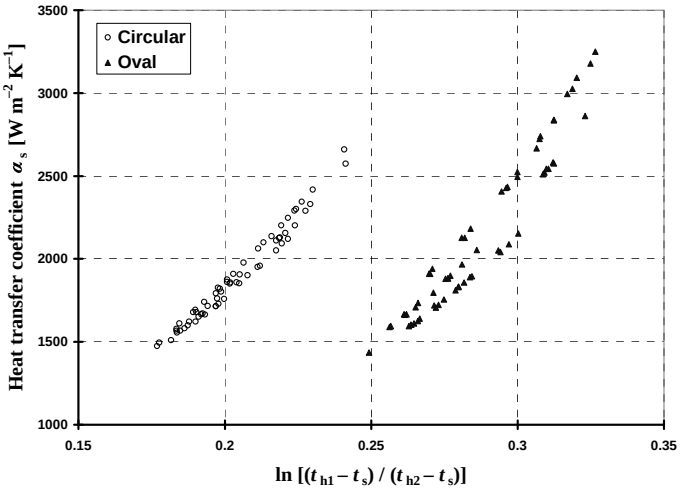

Fig. 4.12. Heat transfer coefficient α_s for the circular and oval tubes.

The mass transfer coefficient K concluded from the measurements is shown in Fig. 4.13, where higher values of K can be seen for the circular tubes. The correlation for the data in this figure gives: $K = 0.077\ v_{\max}^{0.812}$ for the circular tubes, and $K = 0.064\ v_{\max}^{0.706}$ for the oval tubes.

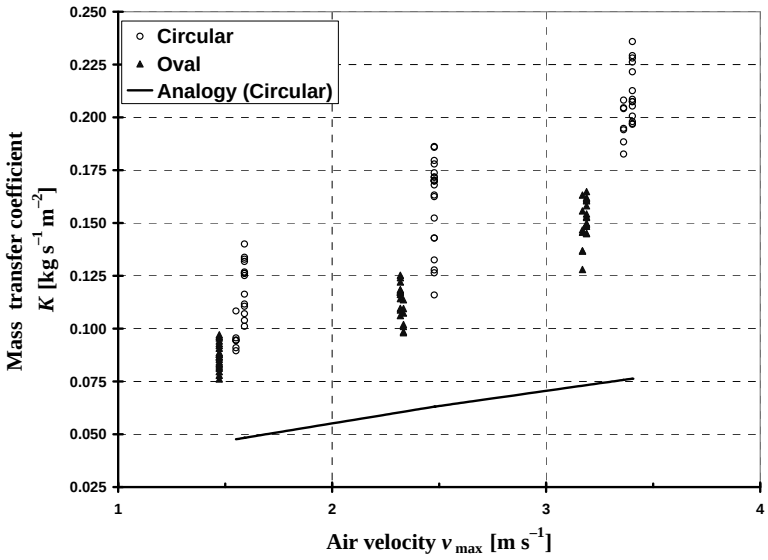

Fig. 4.13. Mass transfer coefficient K for the circular and oval tubes.

The mass transfer coefficient could be concluded from correlations for dry heat transfer according to the heat-mass analogy (ASHRAE, 1997). For the circular tubes, Fig. 4.13 indicates that the heat-mass transfer analogy gives lower K values compared to those obtained from the measurements. Similar behaviour was also noticed by Parker and Treybal (1962) and Dreyer and Erens (1990) according to their test results. Such discrepancies could be attributed to a higher actual contact area produced by water splash and by interaction between air and spray water film.

The friction factor f is calculated from $f = \Delta p / (0.5 \rho v_{max}^2)$ where Δp is the air pressure drop across one tube row in a dry operation. The friction factors for the circular and oval tubes are shown in Fig. 4.14 versus the air Reynolds number Re where the effects of variable air velocity and tube diameter are taken into account ($Re = v_{max} D_o \rho / \mu$). A lower f value that is 46% of that for the circular tubes could be noticed for the oval tubes. This is in accordance with the expectations of a lower pressure drop for oval tubes as a result of their slender shape.

The mass transfer Colburn factor j_m is defined as $j_m = Sh / (Re\ Sc^{1/3})$, where Sh is the Sherwood number and Sc is the Schmidt number. j_m can also be written as $j_m = K\ Sc^{2/3} / (\rho\ v_{max})$. The mass transfer Colburn factor j_m from the experimental measurements is plotted in Fig. 4.14 against the air Reynolds number for both the oval and circular tubes. The average Colburn factor for the oval tubes is 89% of that for the circular tubes.

The thermal-hydraulic characteristics of the tubes can be represented by the ratio of the mass transfer Colburn factor to the friction factor (j_m / f), which is also displayed in Fig. 4.14. From this it can be concluded that the ratio (j_m / f) for the oval tubes is 1.93 to 1.96 times that for the circular tubes in the range of overlap of Re for the two types of tubes.

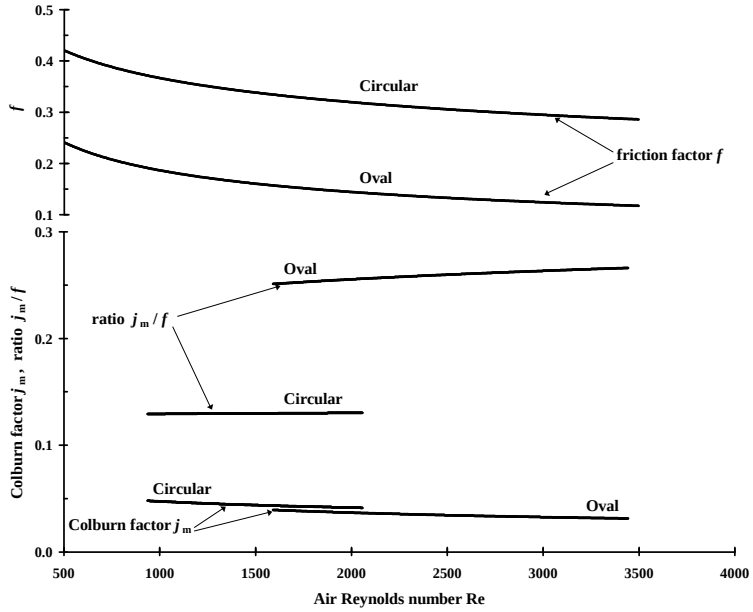

Fig. 4.14. The mass transfer Colburn factor j_m, the friction factor f, and the ratio j_m / f for the circular and oval tubes.

It is concluded that the oval tube has good heat and mass transfer characteristics and better characteristics for the pressure drop, so the combined heat-pressure performance shows favourable features for oval tubes in evaporatively cooled heat exchangers.

The effect of wall material, convective and mass resistances on the total heat transfer

The relative effect of a component resistance could be found by combining all the resistances into one equation. As shown by Fig. 4.15, the total resistance R_{tot} includes the heat convection resistance between hot water and tube wall R_1, the tube wall conduction resistance R_2, the heat convection resistance between tube wall and spray water R_3, and the resistance to mass transfer R_4.

The relation between the saturation air temperature t'_a and the saturation air enthalpy h'_a can be approximated by a straight line, $h'_a = a + b\,t'_a$, where a and b are constants. Using this approximation, and combining the heat and mass transfer Eqs. (3.1 and 3.2) together with Eq. (2.2), the total heat transfer can be written as

$$q = \frac{(\Delta h_a)_{lm}}{b\left[\frac{1}{\alpha_h A_i} + \frac{1}{2\pi k_w L}\ln\left(\frac{D}{d}\right) + \frac{1}{\alpha_s A_t}\right] + \frac{1}{KA_t}} = \frac{(\Delta h_a)_{lm}}{R_1 + R_2 + R_3 + R_4} \tag{4.10}$$

where $(\Delta h_a)_{lm} = \frac{\Delta h_{in} - \Delta h_{out}}{\ln(\Delta h_{in} / \Delta h_{out})}$, $\Delta h_{in} = h_a'(t_{h1}) - h_{a2}$, and $\Delta h_{out} = h_a'(t_{h2}) - h_{a1}$.

It is to note here that $(\Delta h_a)_{lm}$ is a special definition of the log-mean-air enthalpy-difference as it includes $h_a'(t_{h1})$ and $h_a'(t_{h2})$, which are the air saturation enthalpies evaluated at the hot water temperatures at the inlet and outlet of the heat exchanger, respectively.

Equation (4.10) presents the heat transfer rate in terms of the resistances to enthalpy transfer appearing in the denominator, where $R_1 = \frac{b}{\alpha_h}\frac{1}{A_i}$, $R_2 = \frac{b}{2\pi k_w L}\ln\left(\frac{D}{d}\right)$, $R_3 = \frac{b}{\alpha_s A_t}$, $R_4 = \frac{1}{KA_t}$.

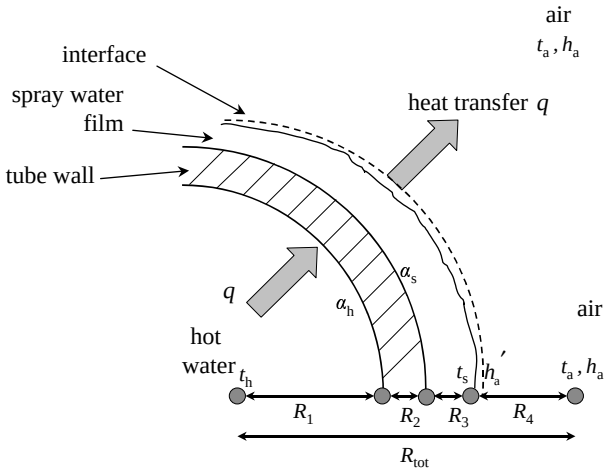

Fig. 4.15. Heat transfer from the hot water to air and the heat and mass resistances.

Calculations are carried out using Eq. (4.10) to see the effect of the tube wall thermal conductivity k_w on the heat transfer for three materials: PVC (0.15 W m^{-1} K^{-1}), carbon steel (50 W m^{-1} K^{-1}), and copper (300 W m^{-1} K^{-1}). The results show that the metallic tubes preserve similar heat transfer rates; while for the plastic tube, it is about 16% of that for the metallic tubes. Therefore, the tubes should be made from conductive materials, while for the extended surfaces, the use of nonconductive materials is possible as was discussed before.

The tested tubes were copper, which means negligible wall resistance. Therefore, the wall material resistance can be omitted from Eq. (4.10). The effect of variation of K or U_o on the total heat transfer q can be determined from the differentiation of Eq. (4.10) with respect to K or U_o, respectively. From which we can find

$$\frac{\mathrm{d}q/q}{\mathrm{d}K/K} = \left(1 + \frac{bK}{U_\mathrm{o}}\right)^{-1} \tag{4.11}$$

$$\frac{\mathrm{d}q/q}{\mathrm{d}U_\mathrm{o}/U_\mathrm{o}} = \left(1 + \frac{U_\mathrm{o}}{bK}\right)^{-1} \tag{4.12}$$

It can be noted that Eqs. 4.11 and 4.12 equal the ratio of the mass transfer resistance and the heat transfer resistance to the total resistance, R_4/ R_{tot} and $(R_1+ R_3)/ R_{tot}$, respectively. In Fig. 4.16, $\frac{\mathrm{d}q/q}{\mathrm{d}K/K}$ is plotted against K obtained from the measurements for the circular and oval tubes. It appears from this figure that the ratio of the mass transfer resistance to the total resistance ranges from 48% to 70%. It can be concluded here that, for this work, no general prediction could be made concerning which one is dominating, the mass transfer resistance or the heat transfer resistance. Despite that K appears to be relatively more effective, the exact effect is dependant on the values of the transfer coefficients for each case.

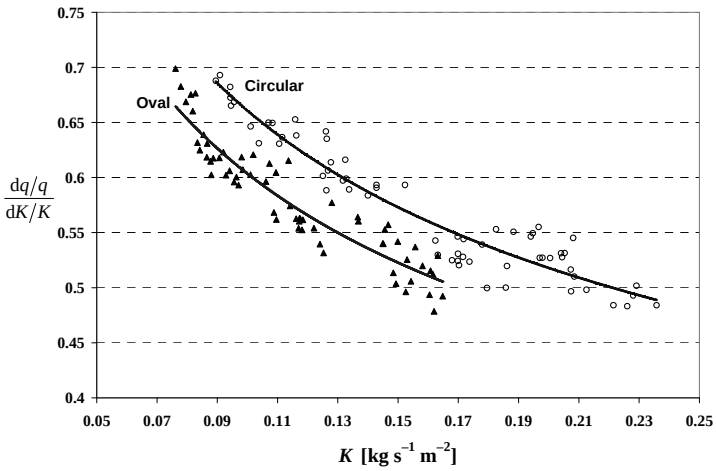

Fig. 4.16. The relative effect of variation of K on the total heat transfer from the experimental measurements.

5 THERMAL-HYDRAULIC PERFORMANCE OF OVAL TUBES IN A CROSS-FLOW OF AIR

The characteristics of oval tubes in ECHEs have been described in Section 4.2. The features of oval tubes will appear clearer in dry heat exchangers. As was presented in the background of this study (Section 1.1), the available literature is inconclusive concerning the expected thermal performance of oval tubes in relation to circular tubes. The objective of Paper V is to experimentally investigate the thermal and hydraulic performance of oval tubes in a cross-flow of air and compare it with that for an equivalent circular tube. Five shapes of oval tubes are investigated.

5.1 Experimental work

Tube dimensions

The dimensions of the tested circular tube and the five oval tubes are indicated in Fig. 5.1. The circular tube outside diameter D_o is 18 mm. The axis ratios (outer major axis c to outer minor axis y) for three of the oval tubes are 1.9, 2.8, and 4, which will be referred to by the nominal values of R = 2, 3, and 4, respectively. The investigation also covers two special oval tube configurations. One is an oval tube R = 3 with two steel wires soldered along the tube at a central angular position of ± 90º. The wire cross-section is semicircular and its height is 1 mm. The profile of the second tube is composed of two identical arcs of a bigger oval shape which is cut at a right angle at the rear. This tube will be referred to as the cut-oval tube. Its minor axis is equal to that of the oval tube R = 3, while its major axis is shorter (c = 23.3 mm). The perimeter of the formed oval tubes was made equal to that of the circular tube (D_o = 18 mm) from which they were formed. This means that the heat transfer will be based on an equal surface area for the tested tubes.

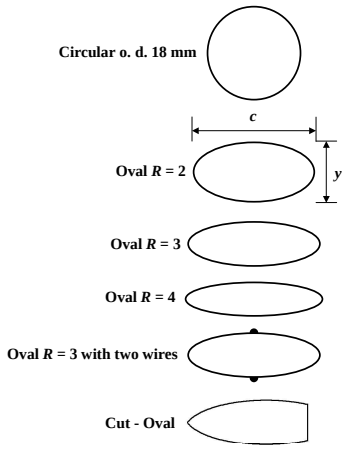

Oval tube	c (mm)	y (mm)	c / y
R = 2	22.2	11.7	1.9
R = 3	24	8.6	2.8
R = 4	25.1	6.3	4
R = 3 with wires	24	8.6	2.8
Cut-oval	23.3	8.6	2.7

Fig. 5.1. Shapes and dimensions of the tested tubes.

Test rigs

A test rig was built for the measurement of heat transfer from the tubes as shown by Fig. 5.2a. The test rig consisted of a low-speed wind tunnel, test section, water system, fan, and measuring instruments.

Air was driven through the wind tunnel and test section by a fan. The wind tunnel length is 1500 mm. Its inlet and outlet sections are square, 800 mm × 800 mm and 400 mm × 400 mm, respectively. The profile of the wind tunnel is a sixth-order polynomial.

The water system comprised an electric heater, pump, water flow meter, electric power meter, and thermocouples. The temperature of the inlet water to the test section was kept at about 70ºC. The water system is insulated from the surroundings. The water system is connected to a copper tube inside which the hot water flows. The copper tube makes four horizontal passes through the test section forming a single array of tubes (Fig. 5.2b). The transversal tube spacing is 80 mm. The hot water was circulated by the pump in a closed circuit. Heat transfer took place from the hot water to the air, which flowed normally to the tubes. The electric power meter was used to measure the power supply to the heater and the pump. For a single array of tubes, as in the current work, Zukauskas (1972) indicated that the heat transfer from a tube in the array is similar to that for a single tube standing alone in the test section. Figure 5.2c shows flow restriction due to the existence of the tube in the channel (the blockage effect).

Air velocity upstream to the tubes V_T was about 1 to 10.5 m s^{-1}, which covers a wide range for general heat transfer applications. Air Reynolds number ($Re_D = V_f D_o \rho / \mu$) was about 1000 to 11000 which implies that the flow was in the lower range of the subcritical external flow.

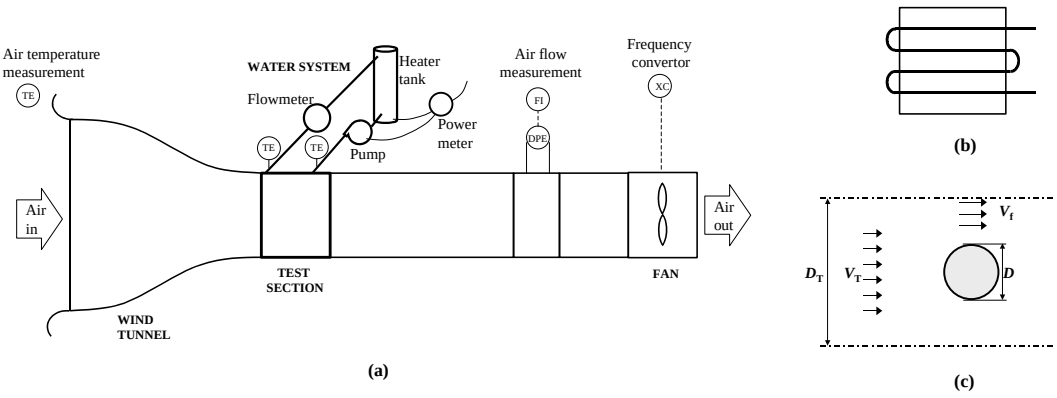

Fig. 5.2. (a) Test rig for the thermal measurement (b) Tube passes (c) Blockage effect on air velocity.

The surfaces of the tubes were polished to eliminate radiation heat transfer. A bright tube has an emissivity of 0.02, which makes its radiation losses negligible.

A simple test rig was constructed to find the drag force F_D for each tube, which was determined from measurements of the force required to keep the tube in its free-suspension position.

5.2 Results and discussion

Heat loss from the insulated hot water system to the surroundings was measured by bypassing the tubes inside the test section and operating the hot water system. The insulation resistance for heat loss to the surroundings was found by measuring the electrical power supply required to keep a steady state temperature for the water.

The overall characteristics of the tubes will be determined from the thermal and hydraulic measurements.

5.2.1 Thermal measurements

The air-side convective heat transfer coefficient for the tube α_a is found from

$$q = \frac{\Delta t_{lm}}{\frac{1}{\alpha_a A_o} + \frac{D_o}{2 k_w A_o} \ln\left(\frac{A_o}{A_i}\right) + \frac{1}{\alpha_H A_i}} \tag{5.1}$$

where q is the rate of heat transfer from hot water to air and Δt_{lm} is the log-mean-temperature-difference which is determined from the temperature measurements for air and water. For a steady state case, the rate of heat transfer q is evaluated from the measured electrical power supply, which is converted into heat, and the insulation heat loss. The tube wall thermal resistance to heat conduction and the internal flow resistance to heat convection are too small, so that the resistance to convective heat transfer from the tube surface to air ($1 / \alpha_a A_o$) dominates. The mean Nusselt number is evaluated from $Nu_D = \alpha_a D_o / k_a$.

5.2.1.1 Heat transfer measurements for the circular tube

Heat transfer measurements were carried out first for the circular tube (18 mm o. d), where it is considered as a reference case for other measurements. Morgan (1975) reviewed more than 100 references for the relation between the Nusselt number Nu_D and the Reynolds number Re_D for a circular cylinder in a cross-flow of air. He proposed correlations of heat transfer in the form $Nu_D = n_1 Re_D^{n_2}$, where the Nu_D is taken for a turbulence free flow and the Re_D is defined in terms of the air free stream velocity V_f.

Morgan (1975) indicated that his proposed correlations are the same as those empirically obtained by Hilpert (1933) when the latter are corrected by using new data for the thermophysical properties of air. The results of the heat transfer measurements for the circular tube from the current work are compared to Morgan's correlations. The characteristics of the tubes are corrected for the blockage effect (solid and wake blockages) and the turbulence effect.

Solid and wake blockages effect

This effect is due to the flow obstruction produced by placing a tube in a channel (Fig. 5.2c). An equation by Vincenti and Graham (1946) is applied that corrects for the solid and wake blockages effect for a circular cylinder of diameter D placed in a closed-throat wind tunnel of diameter D_T. Here D is taken as D_o for the circular tube or y (the outer minor axis) for the oval tubes and D_T is taken as the height of the flow channel per one tube. This equation was also implemented by Morgan (1975). For the data from the current work, this equation indicates that $V_f / V_T = 1.1$ for the circular tube and $V_f / V_T \leq 1.04$ for the oval tubes (where V_f is the free stream velocity of the obstructed flow and V_T is the upstream velocity of air to the test section).

Turbulence intensity effect

Free stream turbulence intensity (Tu) produced by instantaneous fluctuations of air velocity at the test-section was measured by means of a hot-wire anemometer. These measurements indicate that the turbulence intensity ranges from 0.7% to 3.8% for air velocity ranging from 1.1 to 10.8 m s^{-1}. The effect of higher free stream turbulence intensity is a higher heat transfer rate from the tube surface. Correlations presented by Comings et al. (1948) and van der Hegge Zijnen (1957-1958) were considered by Morgan to evaluate the increase in the Nusselt number due to the turbulence intensity in the direction of flow for circular cylinders in the range of $Re_D = 10000$. Those correlations will be considered for the correction of the turbulence effect in the current work. From which, the flow turbulence intensity in this work (Tu = 0.7% to 3.8%) gives an 11% to 27% increase in the Nu_D.

Reference measurement (the circular tube measurements)

Figure 5.3 shows the measurement results for the 18 mm o. d. circular tube and the corrections for the blockage effect and the turbulence effect. For the blockage effect correction, the measurement points for Re_D based on V_T are corrected to higher values based on V_f. The effect of the turbulence intensity on the heat transfer is excluded, which results in a lower Nu_D. The corrected measurement points are shown in relation to Morgan's correlation where the latter involves a maximum uncertainty of ± 5%. As seen in the figure, the corrected measurement points are very close to the correlation. This is a check of the measuring procedure and facilities.

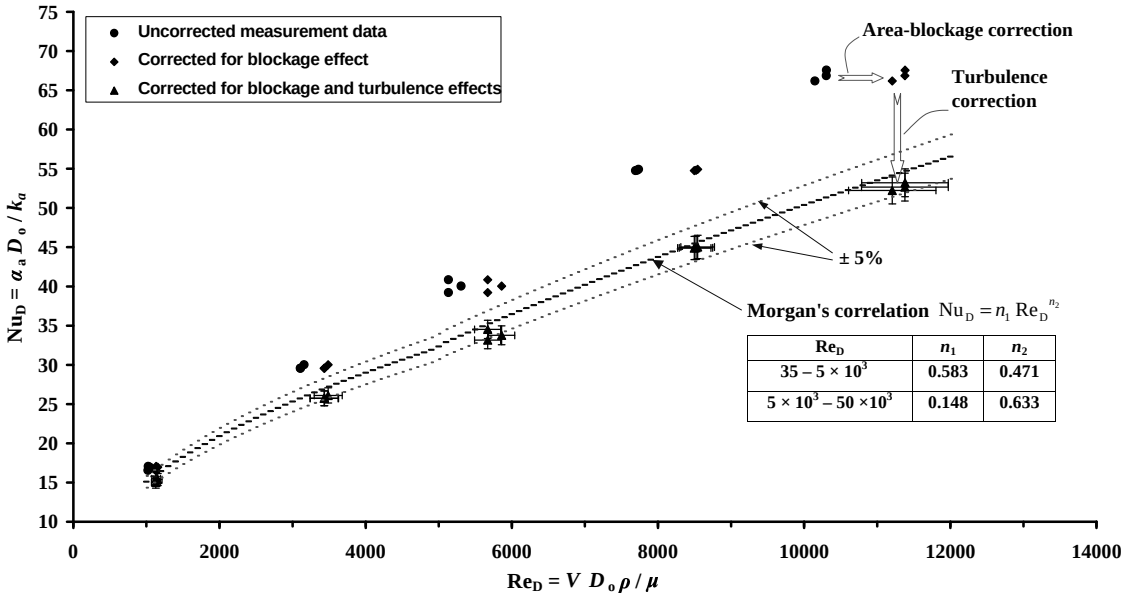

Fig. 5.3. Thermal measurement results for the circular tube (the error bars are for the final corrected points).

5.2.1.2 Heat transfer measurements for the oval tubes

The major axis of the oval tubes was parallel to the direction of the air flow. The oval tubes were formed from 18 mm o. d. copper circular tubes, which, after forming, preserved the same perimeter as the circular tube.

Figure 5.4 shows the Nusselt number for three oval tubes (nominal axis ratios R of 2, 3, and 4) with that for the circular tube. The measurement results are corrected for the effects of area blockage and flow turbulence as before. To compare with the circular tube, the characteristic length in the definition of the Reynolds number (Re_D) and Nusselt number (Nu_D) for the oval tubes is taken to be equal to the outside diameter of the circular tube which has the equivalent perimeter (here D_o = 18 mm). This definition was implemented by Ota et al. (1983, 1984) and Kondjoyan and Daudin (1995). Jacob (1949) referred to a similar definition for noncircular tubes.

It appears from Fig. 5.4 that the differences between the Nu_D for the circular and oval tubes for lower Reynolds numbers (Re_D < 4000) are so small that almost all of the measurement points for the oval tubes are within a ± 5% range around the measurement points for the circular tube. Noting that Re_D < 4000 here corresponds to an air velocity of less than 4 m s^{-1}, which is the range for most air-conditioning applications. While for higher Reynolds numbers (Re_D > 4000), Nu_D for the oval tubes is lower than that for the circular tube and the general trend is that it decreases with the increase of the axis ratio R. At Re_D = 11000, the decrease in Nu_D for the oval tubes from that for the circular tube is 8% for R = 2 and 16% for R = 3 and R = 4. Lower Nu_D for an elliptical cylinder (R = 4) was also reported by Kondjoyan and Daudin (1995) when compared to that for an equivalent circular cylinder.

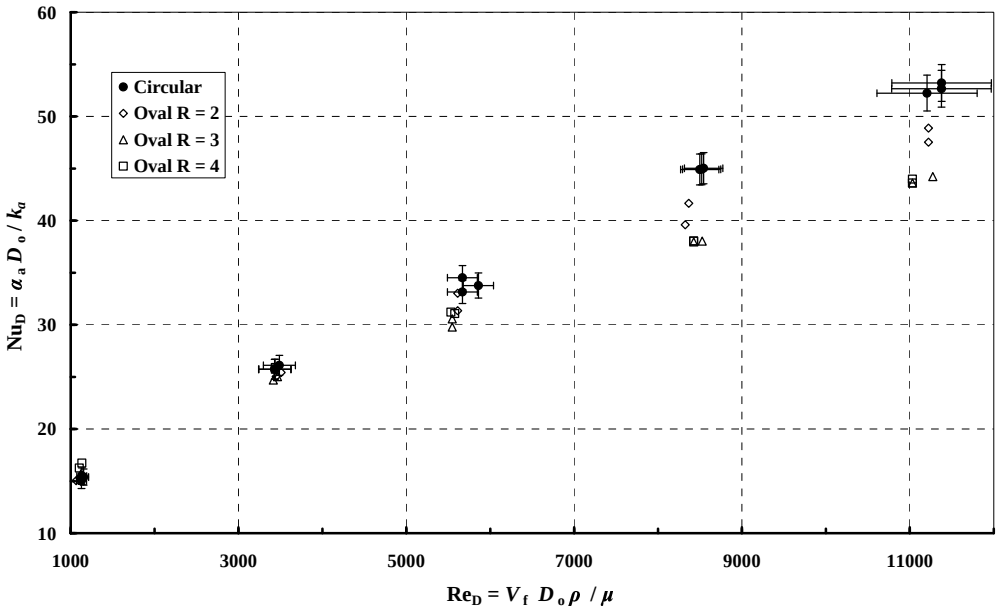

Fig. 5.4. Thermal measurement results for the circular tube and the oval tubes R = 2, 3, and 4 (the error bars are for the circular tube points).

For subcritical flow around a circular tube, separation of the laminar boundary layer occurs at an angle of about 80º due to the expansion in flow area and the adverse pressure gradient. The local Nu is largest at the stagnation point and it decreases with the distance along the surface due to the growth of boundary layer thickness. The local Nu reaches its minimum near the separation point and starts to increase beyond that, but it stays smaller than that for the stagnation point. A similar behaviour will exist for oval tubes.

For external flow around an object, the boundary layer grows thicker as the surface becomes flatter. This explains the decrease of Nu_D for the oval tubes for $Re_D > 4000$. However, the change of the tube geometry from circular to oval for the lower range of the Reynolds numbers ($Re_D < 4000$) seems to have an insignificant effect on Nu_D. It is worthwhile noting that the coefficients of the Morgan's correlations and the Hilpert's corrected correlations change beyond $Re_D = 5000$, which could refer to a change in the heat transfer characteristics for the tube starting from the indicated Re_D. This could have a relation to the change of the thermal behaviour noticed in the measurements from this work for $Re_D > 4000$.

Figure 5.5 shows Nu_D for three oval tubes: the oval tube R = 3, the oval tube R = 3 with the two wires, and the cut-oval tube. The location of the wire is expected to be a little upstream of the separation point for a plain oval tube. Figure 5.5 indicates that these tubes seem to have an almost identical thermal performance.

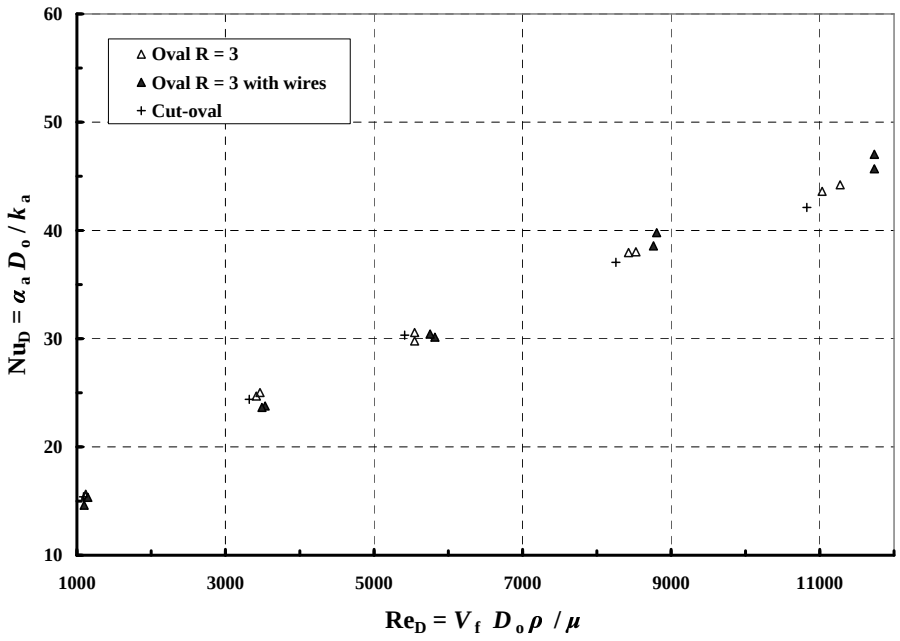

Fig. 5.5. Thermal measurements for the oval tube R = 3, the oval tube R = 3 with the wires, and the cut-oval tube.

5.2.2 Hydraulic measurements

The drag coefficient C_d for each tube is found from the drag force F_d measurements

$$C_d = \frac{F_d}{0.5\,\rho\,v_T^{\,2}\,A_F} \tag{5.2}$$

where A_F is the tube frontal area perpendicular to the free stream direction. The drag measurements for the tubes are presented in Fig. 5.6. They are presented against Re_c, where $Re_c = V_T\,c\,\rho\,/\,\mu$, which is based on the tube chord c (major axis for the oval tubes). It can be seen that C_d for the oval tubes is lower than that for the circular tube, and it decreases with increased oval tube axis ratio R. Table 5.1 shows $C_{d\,avg}$ the average value of the drag coefficient over the investigated range of Re_c for each tube together with that available from the literature for comparable sections.

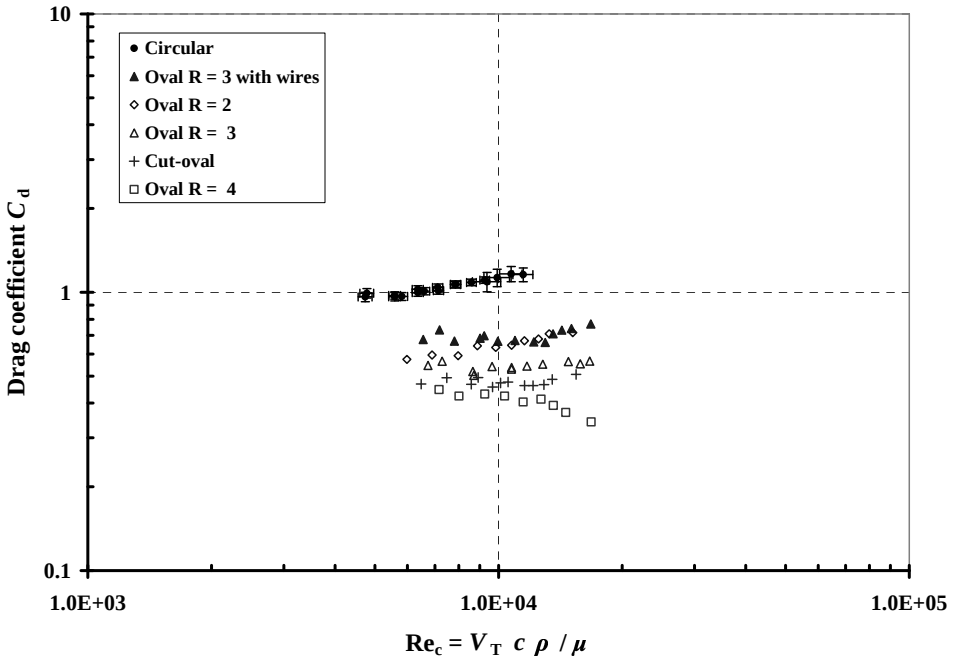

Fig. 5.6. Drag coefficients for the investigated tubes (the error bars are for the circular tube points).

5.2.3 Combined thermal-hydraulic performance of the tubes

The ratio $Nu_D / C_{d\,avg}$ is taken as an indication of the thermal-hydraulic characteristics of the tubes. Figure 5.7 shows this ratio as determined from the measurement data. It can be seen from this figure that the tested oval tubes are better than the circular tube in a combined thermal-hydraulic performance. The tube performance relative to that for the circular tube $\dfrac{(Nu_D / C_{d\,avg})}{(Nu_D / C_{d\,avg})_{circular}}$ has the average values indicated in Table 5.1 over the examined range of Re_D.

In addition to the indicated better combined thermal-hydraulic performance, oval tube heat exchangers are more compact than circular tube heat exchangers, which means a higher heat transfer area per volume. These results for single tubes are indications for possible future work on bundles of plain or finned oval tubes with different heat transfer enhancement objects on the surface.

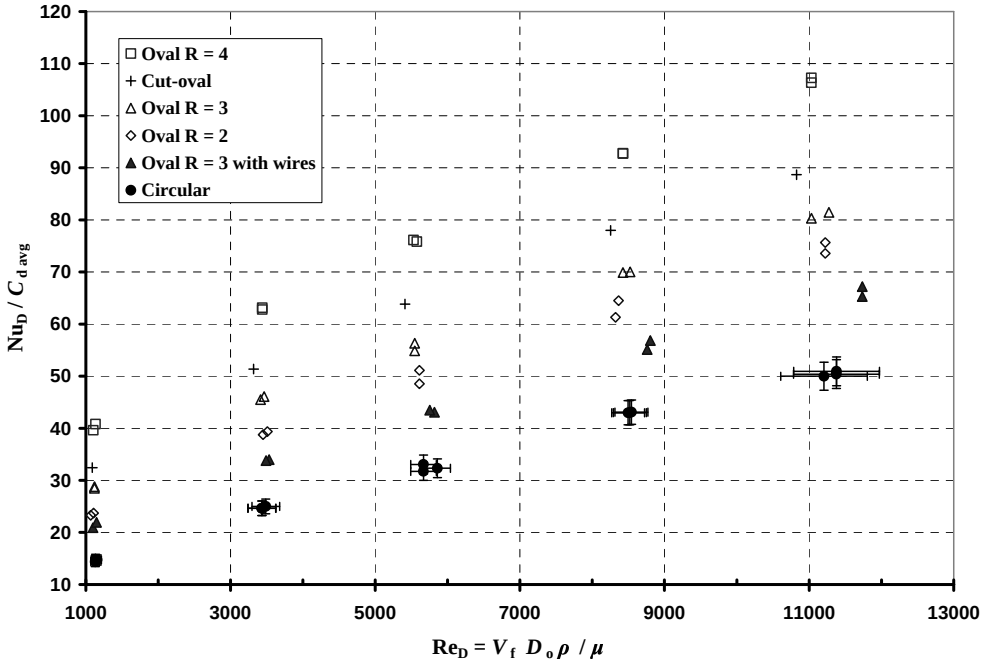

Fig. 5.7. The combined thermal-hydraulic performance for the tubes (the error bars are for the circular tube points).

Table 5.1. The drag coefficient $C_{\mathrm{d\,avg}}$ from the measurements and literature and the ratio $\dfrac{(\mathrm{Nu_D}/C_{\mathrm{d\,avg}})}{(\mathrm{Nu_D}/C_{\mathrm{d\,avg}})_{\mathrm{circular}}}$ from the measurements data.

	$C_{\mathrm{d\,avg}}$		$\dfrac{(\mathrm{Nu_D}/C_{\mathrm{d\,avg}})}{(\mathrm{Nu_D}/C_{\mathrm{d\,avg}})_{\mathrm{circular}}}$
	Measured	**Literature**	
Circular	1.05	1[a], 1.2[b]	1.0
Oval *R* = 2	0.65	0.6[c]	1.6
Oval *R* = 3	0.54	0.43[c]	1.8
Oval *R* = 4	0.41	0.35[c]	2.5
Oval *R* = 3 with wires	0.70	–	1.3
Cut-oval	0.48	–	2.1

[a] Knudsen and Katz (1958), [b] Morgan (1975), [c] Hoerner (1965).

6 CONCLUSIONS

CWCTs in conjunction with chilled ceilings can be used for the cooling of buildings. The performance of CWCTs is modelled with a computational model where the tower is divided into volumetric elements and the variable spray water temperature is considered. The tower model is integrated into a global cooling system simulation program which could include models for other components of the cooling system (e.g. transient building model, chilled ceiling model, system control etc.). To simulate the tower performance under various operating conditions, the transfer coefficients of the tower are introduced from test measurements. Cooling tower modelling allows the study of the geometry and operating conditions of the CWCT where the objective is to achieve the heat transfer duty with a high value of COP.

Simplified analytical models, which are obtained by assuming a constant spray water temperature, are also investigated. Results of simplified models appear to be close to those for the computational model. The results of the simplified CWCT model are incorporated with CFD to assess the effects of air flow distribution inside the tower on its performance. This shows that CFD is a useful tool for the analysis of the effects of variations in air and spray water flow patterns inside the tower on its performance.

The utilisation of plate-finned tubes in an ECHE is experimentally investigated and the performance is compared to that of plain tubes. Despite that the mass transfer coefficient could be lower for the finned tubes, a considerable increase in the heat transfer takes place when using the plate-finned tubes which is due to the larger total wetted area. The increase is from 92% to 140%. For a specific volume, the combined thermal-hydraulic characteristics show a higher rate of heat transfer for the finned tubes with a close energy index.

The thermal and hydraulic performance of circular and oval tubes in an ECHE is compared experimentally. The axis ratio R for the oval tube is 3.085. The measurement results show that the average mass transfer Colburn factor j_m for the oval tube is 89% of that for the circular tube, while the friction factor f for the oval tube is 46% of that for the circular tube. Combining the thermal and the hydraulic characteristics of the tubes, the oval tube shows higher values for (j_m / f), which is 1.93 to 1.96 times that for the circular tube. It could be concluded that the oval tube has good heat and mass transfer characteristics and better characteristics for the pressure drop, so that the combined heat-pressure performance shows favourable features for oval tubes in ECHEs.

For the heat transfer from five dry oval tubes in a cross-flow of air, Nu_D at Reynolds number $Re_D < 4000$ appears to be close to that for the equivalent circular tube. This range corresponds to an air velocity < 4 m s^{-1}, which is the velocity for most air-conditioning applications. For a higher Re_D, the Nu_D for the oval tubes appears to be lower than that for the circular tube and it decreases with the increase in the axis ratio R. At $Re_D = 11000$, the decrease in Nu_D for the oval tubes compared to that for the circular tube is 8% for $R = 2$ and 16% for $R = 3$ and $R = 4$. The drag coefficients $C_{d\ avg}$ for oval tubes are lower than that for the circular tube. The investigated oval tubes appear to

have better combined thermal-hydraulic performance compared to that for the circular tube. The ratio of (Nu_D /$C_{d\ avg}$) for the oval tubes to that for the circular tube is: 1.6 for R = 2, 1.8 for R = 3, 2.5 for R = 4, 1.3 for the oval tube with the wires, and 2.1 for the cut-oval tube.

Because of their smaller face area, oval tube heat exchangers are more compact than circular tube heat exchangers, which means the utilisation of a larger heat transfer area in a specified volume. Added to their better combined thermal-hydraulic performance, these features indicate encouraging characteristics for using oval tubes in dry and wet heat exchangers.

It is worthwhile noting that the several expressions for the energy efficiency implemented in this study (COP, energy index E, j_m / f, and Nu_D /$C_{d\ avg}$) have shown similar trends in the results and led to consistent conclusions. The results of this study are indicative for general applications of CWCTs, wet finned tubes, and wet and dry oval tubes. The exact performance for any other specific case is dependant on the geometry and operating conditions.

REFERENCES

ASHRAE (1992). Systems and Equipment, American Society of Heating, Refrigeration and Air Conditioning Engineers, USA.

ASHRAE (1997). Fundamentals, American Society of Heating, Refrigeration and Air Conditioning Engineers, USA.

Bolher A, Fleury E, Millet JR, Marchio D, Stabat P (2002). Guidance and tools for chilled ceilings combined with a wet cooling tower, EPIC AIVC Conference 2002, Lyon, France, 413–418.

Brauer H (1964). Compact heat exchangers, Chemical and Process Engineering **45** (8): 451–460.

Castiglia D, Balabani S, Papadakis G, Yianneskis M (2001). An experimental and numerical study of the flow past elliptic cylinder arrays, Proceedings of the Institution of Mechanical Engineers, Journal of Mechanical Engineering Science **215** Part C (11): 1287–1301.

CIBSE (2000). Minimising the risk of Legionnaires disease, TM 13, CIBSE, London.

Comings EW, Clapp JT, Taylor JF (1948). Air turbulence and transfer processes. Flow normal to cylinders, Ind. Eng. Chem. **40**: 1076–1082.

Costelloe B, Finn D (2003). Experimental energy performance of open cooling towers under low and variable approach conditions for indirect evaporative cooling in buildings, Building Service Engineering Research and Technology **24** (3): 163–177.

Dreyer AA, Erens PJ (1990). Heat and mass transfer coefficient and pressure drop correlations for a crossflow evaporative cooler, Proceedings of the Ninth International Heat Transfer Conference, Hemisphere Publ Corp, New York, USA, Vol. 6, 233–238.

Erens PJ (1988). Comparison of some design choices for evaporative cooler cores, Heat Transfer Engineering **9** (2): 29–35.

Erens PJ, Dreyer AA (1988). An improved procedure for calculating the performance of evaporative closed circuit coolers, The 25th National Heat Transfer Conference, Houston, AIChE symposium series **84**: 140–145.

Facão J, Oliveira AC (1999). Performance tests of CWCT: Experimental results. ECOCOOL project report.

Facão J, Oliveira AC (2000). Thermal behaviour of closed wet cooling towers for use with chilled ceilings, Applied Thermal Engineering **20:** 1225–1236.

Finlay IC, Harris D (1984). Evaporative cooling of tube banks, International Journal of Refrigeration **7** (4): 214–224.

FLUENT (1995). *User's Guide*. Fluent Inc., USA.

Gan G, Riffat SB (1999). Numerical simulation of closed wet cooling towers for chilled ceiling systems, Applied Thermal Engineering **19** (12): 1279–1296.

Gan G, Riffat SB, Shao L, Doherty P (2001). Application of CFD to closed-wet cooling towers, Applied Thermal Engineering **21** (1): 79–92.

Hilpert R (1933). Forschung Gebiete Ingenierwes **4:** 215–224.

Hoerner FS (1965). Fluid Dynamic Drag.

Incropera FP, DeWitt DP (1996). Fundamentals of Heat and Mass Transfer, Fourth edition, John Wiley and Sons,

Jacob M (1949). Heat Transfer, Vol. 1, Wiley, New York.

Jang JY, Yang JY (1998). Experimental and 3-D numerical analysis of the thermal-hydraulic characteristics of elliptic finned-tube heat exchangers, Heat Transfer Engineering **19** (4): 55–67.

Jang JY, Wang ZG (2001). Heat and mass transfer performance of closed-type towers, Advances in Computational Heat Transfer II, Proceedings of a Symposium by the International Centre for Heat and Mass Transfer, Queensland, Australia, 269-276.

Khan MG, Fartaj A, Ting D S-K (2004). An experimental characterization of cross-flow cooling of air via an in-line elliptical tube array, International Journal of Heat and Fluid Flow **25** (4): 636–648.

Knudsen JG, Katz DL (1958). Fluid Dynamics and Heat Transfer, McGraw-Hill Co.

Kondjoyan A, Daudin JD (1995). Effects of free stream turbulence intensity on heat and mass transfer at the surface of a circular cylinder and an elliptical cylinder axis ratio 4, International Journal of Heat and Mass Transfer **38** (10): 1735–1749.

Koschenz M (1995). Model for closed circuit evaporative cooling tower, IBPSA International Building Performance Simulation Association, 4th Int. Conf., Madison, Wisconsin, USA.

Kried DK, Johnson BM, Faletti DW (1978). Approximate analysis of heat transfer from the surface of a wet finned heat exchanger, ASME paper 78-HT-26.

Leidenfrost W, Korenic B (1986). Principles of evaporative cooling and heat transfer augmentation. In: Cheremisinoff NP, Handbook of Heat and Mass Transfer, Vol. 1, Gulf Publishing, Houston, 1025-1063.

Liu R, Fartaj A, Ting D S-K (2003). An experimental study on cross-flow cooling via an elliptical tube array, The 6th ASME-JSME Thermal Engineering Joint Conference.

Merkel F (1925). Verdunstungskuehlung, VDI Forschungsarbeiten No. 275, Berlin.

Merker GP, Hanke H (1986). Heat transfer and pressure drop on the shell-side of tube-banks having oval-shaped tubes. International Journal of Heat and Mass Transfer **29** (12): 1903–1909.

Milosavljevic N, Heikkilä P (2001). A comprehensive approach to cooling tower design, Applied Thermal Engineering **21** (9): 899–915.

Mizushina T, Ito R, Miyashita H (1967). Experimental study of an evaporative cooler, International Chemical Engineering **7** (4): 727–732.

Mizushina T, Ito R, Miyashita H (1968). Characteristics and methods of thermal design of evaporative cooler, International Chemical Engineering **8** (3): 532–538.

Morgan VT (1975). The overall convective heat transfer for smooth circular cylinders, Advances in Heat Transfer **11**: 199–264.

Niitsu Y, Naito K, Anzai T (1969). Studies on characteristics and design procedure of evaporative coolers, Journal of SHASE Japan **43** (7): 581–590.

Nishiyama H, Ota T, Matsuno T (1987). Forced convection heat transfer from elliptic cylinders in tandem arrangement. Proceedings of the 1987 ASME-JSME Thermal Engineering Joint Conference, Honolulu, USA **4**: 151–157.

Oliveira A, Facão J, Afonso C and others (2000). Chilled ceilings: An ecological cooling system using closed wet cooling towers, Proceedings of ROOMVENT 2000, International Conference on Air Distribution in Rooms, Reading, UK.

Ota T, Aiba S, Tsuruta T, Kaga M (1983). Forced Convection Heat Transfer from an Elliptic Cylinder of Axis Ratio 1:2, Bulletin of JSME **26** (212): 262–267.

Ota T, Nishiyama H, Taoka Y (1984). Heat transfer and flow around an elliptic cylinder, International Journal of Heat and Mass Transfer **27** (10): 1771–1779.

Ota T, Nishiyama H (1986). Flow around two elliptic cylinders in tandem arrangement, Journal of Fluids Engineering, Transactions of the ASME **108** (1): 98–103.

Parker RO, Treybal RE (1962). The heat mass transfer characteristics of evaporative coolers, Chemical Engineering Progress Symposium **57** (32): 138–149.

Peterson D, Glasser D, Williams D, Ramsden R (1988). Predicting the performance of an evaporative condenser, Journal of Heat Transfer, Trans. of ASME **110**: 748–753.

Poppe M (1973). Heat and mass transfer at counter and cross flow evaporation cooling, VDI Forschungsheft **39** (560).

Reiher H (1925). Handbuch der Experimental Physik, Vol. 9, Part. 1, Leipzig.

Saboya SM, Saboya FEM (2001). Experiments on elliptic sections in one-and two-row arrangements of plate fin and tube heat exchangers, Experimental Thermal and Fluid Science **24** (1-2): 67–75.

Salazar E, Gonzalez JJ, Lopez De Ramos A, Pironti F, Gonzalez-Mendizabal D (1997). Evaluation of the heat transfer coefficient in a bank of elliptic tubes, American Institution of Chemical Engineers Symposium Series, Heat Transfer **314**: 185–190.

Schmidt TE (1949). Heat transfer calculations for extended surfaces, Refrigerating Engineering **4**: 351–357.

Schubauer GB (1936). Air flow in a separating laminar boundary layer, NACA report No. 527.

Schulenberg FJ (1966). Finned elliptical tubes and their application in air-cooled heat exchangers, Transactions of the ASME **88**: 179–190.

Sprecher P, Gasser B, Böck O, Kofoed P (1995), Control strategy for cooled ceiling panels, ASHRAE Trans. **101** (2): 711–716.

Sprecher P, Gasser B, Koschenz M, Kofoed P (1996). NENOP Energieoptimaler Betrieb Von Kuehldecken. Technical Report 575, Swiss National Energy Research Fund, Switzerland.

Sprecher P, Borth J, Niessen R (2000). Cooler ceilings with less energy, Sulzer Technical Review, No 1: 10–11.

Threlkeld JL (1970). Thermal Environmental Engineering, 2nd Ed, Prentice-Hall, N.J.

TRNSYS (1996). Transient System Simulation Program, Univ. of Wisconsin, Madison, USA.

van der Hegge Zijnen BG (1957–1958). Heat transfer from horizontal cylinders to a turbulent air flow, Appl. Sci. Res. Sect. **A7**: 205–223.

Vincenti WG, Graham DJ (1946). NACA Tech. Rep. No. 849.

Zalewski W, Gryglaszewski PA (1997). Mathematical model of heat and mass transfer processes in evaporative fluid coolers, Chemical Engineering and Processing **36**: 271–280.

Zukauskas A (1972). Heat transfer from tubes in cross flow, Advances in Heat Transfer **8**: 93–160.

ORIGINAL PUBLICATIONS

I Theoretical and computational analysis of closed wet cooling towers and its applications in cooling of buildings

II Simplification of analytical models and incorporation with CFD for the performance prediction of closed wet cooling towers

III Performance investigation of plain and finned tube evaporatively cooled heat exchangers

IV Performance investigation of plain circular and oval tube evaporatively cooled heat exchangers

V Thermal-hydraulic performance of oval tubes in a cross-flow of air